Recapitulation of the EEF1A2 D252H neurodevelopmental disorder-causing missense mutation in mice reveals a toxic gain of function

Recapitulation of the *EEF1A2* D252H neurodevelopmental disorder-causing missense mutation in mice reveals a toxic gain of function.

Faith C.J. Davies[1,2], Jilly E. Hope[1], Fiona McLachlan[1], Grant F. Marshall[1], Laura Kaminioti-Dumont[1], Vesa Qarkaxhija[1], Francis Nunez[1], Owen Dando[2,3], Colin Smith[4], Emma Wood[2,3], Josephine MacDonald[1], Oliver Hardt[2,5] and Catherine M. Abbott[1,2*]

1. Centre for Genomic & Experimental Medicine, MRC Institute of Genetics and Molecular Medicine, University of Edinburgh, Western General Hospital, Crewe Road, Edinburgh EH4 2XU, United Kingdom

2. Simons Initiative for the Developing Brain, University of Edinburgh, Edinburgh EH8 9XD, United Kingdom

3. Centre for Discovery Brain Sciences, University of Edinburgh, Edinburgh EH8 9XD, United Kingdom

4. Academic Department of Neuropathology, Centre for Clinical Brain Sciences, Chancellor's Building, Little France, Edinburgh, EH16 4SB, United Kingdom

5. Department of Psychology, 1205 Dr Penfield Avenue, McGill University, Montreal, QC, H3A 1B1, Canada

* to whom correspondence should be addressed

Centre for Genomic and Experimental Medicine

MRC IGMM, University of Edinburgh, Western General Hospital Crewe Road, Edinburgh, EH4 2XU

Phone +44 131 651 8745

Email C.Abbott@ed.ac.uk

Abstract

Heterozygous *de novo* mutations in *EEF1A2*, encoding the tissue-specific translation elongation factor eEF1A2, have been shown to cause neurodevelopmental disorders including often severe epilepsy and intellectual disability. The mutational profile is unusual; ~50 different missense mutations have been identified but no obvious loss of function mutations, though large heterozygous deletions are known to be compatible with life. A key question is whether the heterozygous missense mutations operate through haploinsufficiency or a gain of function mechanism, an important prerequisite for design of therapeutic strategies. In order both to address this question and to provide a novel model for neurodevelopmental disorders resulting from mutations in *EEF1A2*, we created a new mouse model of the D252H mutation. This mutation causes the eEF1A2 protein to be expressed at lower levels in brain but higher in muscle in the mice. We compared both heterozygous and homozygous D252H and null mutant mice using behavioural and motor phenotyping alongside molecular modelling and analysis of binding partners. Although the proteomic analysis pointed to a loss of function for the D252H mutant protein, the D252H homozygous mice were more severely affected than null homozygotes on the same genetic background. Mice that are heterozygous for the missense mutation show no behavioural abnormalities but do have sex-specific deficits in body mass and motor function. The phenotyping of our novel mouse lines, together with analysis of molecular modelling and interacting proteins, suggest that the D252H mutation results in a gain of function.

Introduction

Developmental and epileptic encephalopathies (DEE) have profound effects on neurodevelopment and are frequently associated with intellectual disability and autism (2). DEEs are now regarded as a genetically heterogeneous group of disorders, predominantly resulting from dominant *de novo* mutations, leading to stratification into groups of what are, essentially, individually rare diseases. Whilst this genetic granularity will ultimately be helpful in terms of precision medicine, the fact remains that over a third of patients with any form of epilepsy remain refractory to treatment with anti-epileptic drugs (AEDs). It has been argued that the reliance on induced seizure models in animals for testing AEDs has limited progress, and that genetic models of epilepsy will be needed for pharmacological advances (3). Furthermore, whilst genetic stratification is crucial in terms of treatment strategies, the vast majority of individuals with a precise genetic diagnosis are still young. This means that the long-term effects of mutations have yet to be established, leaving families with very limited prognostic information for the effects of mutations in a given gene.

One cause of early onset epilepsy that has been established in the last decade is the mutation of a gene called *EEF1A2*. There have now been numerous reports of *de novo* missense mutations in *EEF1A2* associated with neurodevelopmental disorders (4-13). Surprisingly, although there are now ~50 different missense mutations in *EEF1A2* in children with epilepsy, severe intellectual disability and/or autism, no clear loss of function mutations (frameshifts, deletions, nonsense) have ever been identified. On the other hand, heterozygous deletions spanning *EEF1A2* and neighbouring genes have been described and are compatible with life (14, 15). This unusual mutational profile suggests that each missense mutation may operate through a gain of function or dominant negative mechanism, but the facts that there are so many individual mutations, and that they are spread throughout the gene, makes the elucidation of underlying mechanisms a challenge.

The *EEF1A2* gene encodes eEF1A2, a translation elongation factor responsible for the GTP-dependent delivery of aminoacylated tRNAs to the ribosome. This GTP exchange mechanism is facilitated by the eEF1B complex (16). Whilst most translation factors are ubiquitously expressed, consistent with their housekeeping function, eEF1A is found as two independently encoded, tissue-specific variants.

Initially, eEF1A1 is expressed ubiquitously throughout development but becomes downregulated in postnatal neurons and muscle (both skeletal and cardiac), eventually being completely replaced in these cell types by eEF1A2 (17, 18). This process is complete at about 21 days after birth in the mouse; data from humans is scarce, but analysis of transcriptional profiles in the human prefrontal cortex suggests that eEF1A1 reaches its lowest point between 6 months and 2 years, with eEF1A2 peaking in expression by 6 months (http://braincloud.jhmi.edu/plots/) (19). Mice homozygous for a spontaneously occurring deletion in the *Eef1a2* gene (wasted, gene symbol *wst*) develop muscle wasting and neurodegeneration of the motor neurons in the spinal cord with concomitant gliosis, dying by 25-28 days (20). The wasted mutation is a 15.8 kb deletion of the promoter and first exon of the *Eef1a2* gene and is a complete null (20). On the other hand, mice heterozygous for the wasted deletion live a normal lifespan with no signs of neurodegeneration even at 21 months (21). Human and mouse eEF1A2 proteins are almost identical, with only one amino acid difference.

We previously used CRISPR/Cas9 gene editing to recreate in mice the most common epilepsy-causing missense mutation seen in humans, G70S (22). We were unable to create a breeding colony of G70S mice as all founders carrying the mutation were G70S/- compound heterozygotes and died by ~four weeks. The only G70S-carrying animal without a deletion was homozygous for the missense mutation and had to be culled at 18 days, earlier than the stage at which complete null mice start to show any signs of the disorder. Whilst this result was compatible with the idea that the G70S mutation confers a gain of function on the eEF1A2 protein, it was of course impossible to draw robust conclusions from a single animal. We also note that many of the founder animals with biallelic deletions of eEF1A2 had spontaneous fatal seizures; this phenomenon had not been documented in the original wasted mouse line, which was on a mixed genetic background, so the seizure incidence was presumably influenced by the genetic background (C57BL/6) of the CRISPR-derived mice.

We now report the generation of a new mouse line expressing a different missense mutation in eEF1A2, D252H. The D252H mutation has been described twice as a cause of neurodevelopmental disorders, once in the published literature (6) and once in the Decipher database (https://decipher.sanger.ac.uk/). The mutation is predicted by each of a range of computational tools to be damaging (23). Both affected

individuals have severe developmental delay, ID and autism but no or mild, well-controlled epilepsy. We therefore opted to recreate the D252H mutation in mice on the basis that it had occurred in more than one child, was in a favourable position for repair template design, and was unlikely to give rise to fatal seizures in young mice. With this approach, we aimed to have surviving heterozygous mice with which to generate breeding lines, to model neurodevelopmental disorders resulting from mutations in eEF1A2, and to be able to study behavioural and other phenotypic consequences of missense mutations in both heterozygotes and homozygotes.

We further hypothesised, based on the lack of clear loss of function (deletion, frameshift) clinical mutations in humans, that the D252H mutation would cause a gain of function. We were able to harness the power of CRISPR/Cas9 gene editing in the mouse to create both missense and null mutations in eEF1A2 on the same genetic background. This enabled us to make direct comparisons of the resulting phenotypes in order to test the hypothesis that the D252H mutation resulted in a gain of function. Coupling our results from mice with molecular modelling and our analysis of interacting proteins, we deduce that the D252H mutation results in a gain of function.

Results

The D252H mutation prevents binding to eEF1B

The position of the pathogenic D252H mutation on the eEF1A2 protein is shown in Figure 1a, where it can be seen to overlap with the mapped binding site for the GTP exchange factor eEF1B (1, 6). To evaluate the effect of the mutation on the eEF1A2 interactome we transiently transfected SHSY5Y human neuroblastoma cells with V5 tagged cDNA constructs of human wild type eEF1A2 and human eEF1A2 containing the D252H mutation respectively, in parallel with a vector only control. After 48 hours cell pellets were collected, immunoprecipitated with anti-V5 antibody and the resulting peptides analysed using label-free quantification mass spectrometry (LFQ-MS). The most significant change in binding resulting from the D252H mutation was a ~500 fold decrease in each of eEF1B2, eEF1D, eEF1G and VARS (Figure 1b and supplementary table S1). Together, these proteins make up the eEF1B complex that is responsible for GTP exchange on eEF1A. This apparent loss of binding is consistent with the position of the mutation on the eEF1A2 protein relative to the eEF1B binding (Figure 1a). The results of the LFQ-MS were validated by co-immunoprecipitation (Figure 1c) which showed no detectable binding of the eEF1B complex to eEF1A2 carrying the D252H missense mutation. In contrast, eEF1A2 with a different pathogenic mutation, G70S (which results in epileptic encephalopathy), showed similar levels of eEF1B subunit binding to WT eEF1A2. These results suggested a possible loss of function of the D252H mutation; in order to test this in a meaningful physiological context we set out to recreate the mutation in mice.

CRISPR-Cas9 gene editing: design and establishment of breeding lines

We used CRISPR/Cas9 genome editing to change a single base c.G754C (p.D252H) within the mouse *Eef1a2* gene. We designed a pair of gRNAs that would target *Eef1a2* in the region of the desired mutation (Figure 2a), and two separate 200nt single-stranded oligonucleotide (ssODN) repair templates that spanned 100 nucleotides either side of the desired mutation site (supplementary figure S2a). The

first ssODN was equivalent to the wild-type sequence of *Eef1a2* apart from silent mutations at the two PAM-sites, designed to prevent further cutting of the genome after integration

The second ssODN contained both the silent PAM-site mutations and the c.G754C single base change which would encode the D252H mutation when incorporated. The purpose of co-injecting a wild-type repair template alongside the mutant template was to decrease the risk of generating mice with biallelic mutations in *Eef1a2*, as these would not be likely to survive long enough to establish a breeding colony (22).

The two repair templates, together with the pair of gRNAs and Cas9 nickase RNA, were micro-injected into single cell mouse embryos, resulting in the birth of 28 mice (Figure 2b). Two of these founder mice carried the desired mutation on one allele and wild-type sequence on the other (Figure 2c), and are thus referred to as D252H/+. These D252H/+ founders were used to establish two separate breeding lines carrying the D252H mutation. Initial characterisation was performed on homozygous mice from each line independently. There were no significant differences between lines in either weight or neuroscore measured at P21 (supplementary figure S2b and c) so subsequent analysis was carried out using combined data from both lines.

Abundance of eEF1A2 is decreased in brain and increased in muscle of mutant mice

The D252H mutation results in a dose-dependent decrease in brain eEF1A2 protein levels (Figure 2g, 2h). The level of eEF1A2 in the brains of D252H/+ mice is ~80% of that seen in WT littermates, and the abundance in D252H/D252H brain is ~60% of that seen in WT mice, a statistically significant difference ($p=0.0006$ unpaired two tailed t test). There is no significant difference in expression at the RNA level across all three genotypes (Figure 2d and S3c) using 1-way ANOVA, suggesting that the mutant protein is likely to be less stable in brain than the WT protein. In contrast, the level of eEF1A2 in the muscle of mutant animals is the same in D252H/+ heterozygotes as in their wild-type littermates, but is ~1.6 times higher in D252H/D252H mice (figure 2e, 2f) ($p=0.0002$ unpaired two-tailed t test).

No significant difference in expression levels was seen between male and female mice within any genotype (supplementary figure S3a and b).

D252H/+ mice weigh less than wild-type littermates and show neurological deficits

Male and female D252H/+ mice initially follow the same weight growth curve as their WT littermates (Figure 3a and 3d). From postnatal day 14 - 21, however, they consistently weigh ~10% less than their wild-type littermates (Figure 3b and 3e); male D252H/+ vs +/+, p=0.0001; female D252H/+ vs +/+, p= 0.0018. This difference was also apparent in adult mice of both sexes at 2 months: male D252H/+ mice weigh 5% less than wild type littermates, (p=0.009) and female D252H/+ mice weigh 10% less than their wild type littermates (p=0.001). In contrast, the weights of heterozygous null animals are not significantly different from their wild type littermates (Figure S8a and b).

Since the switch from eEF1A1 to eEF1A2 occurs throughout the first 3-4 weeks of postnatal life in mice, and homozygosity for null mutations is lethal by 4 weeks, we needed to develop a scoring system that would allow us to distinguish the phenotypic consequences of any mutation in young mice. In order to quantify the temporal progression of any neurological abnormalities we used an adaptation of the phenotype scoring system described by Guyenet et al.(25) in which four tests (degree of hind limb clasping, gait, kyphosis and ability to walk along a ledge), are each given a score between 0 and 3. Criteria for each score are given in the supplementary methods 1. The combined neuroscore, obtained by adding together the four individual test scores, gives a measure of phenotypic severity. This neuroscore is particularly useful for pre-weaning mice as it can be easily applied daily from P16, when mice are ear notched and genotyped.

Both male and female D252H/+ mice display marginally but significantly worse neuroscores than wild-type littermates between P16 and P23, indicating a small but detectable neurological deficit in young D252H/+ mice (Figure 3g and h; male D252H/+ vs +/+, p=0.0006; female D252H/+ vs +/+, p= 0.0001) which resolves with age (Figure 3i) (possibly due to training). No such neurological deficit is seen in heterozygous null animals (Figure S8c and d).

D252H/+ mice show reduced grip strength

As both known human patients with D252H mutations have microcephaly, gross brain morphology of 60 day old D252H/+ mice was measured by taking coronal slices of PFA-fixed brain at defined locations relative to the Bregma, and comparing relative contribution of each layer of the cortex to overall cortical thickness. No reductions in head size nor gross brain morphology were found between D252H/+ mice and wild-type littermates (supplementary figure S4). Female D252H/+ mice have slightly higher brain to body weight ratios than wild type littermates (Figure 4a) due to their brains weighing 96% that of wild type littermates' brains, but bodies weighing 90% that of their wild type littermates'. Male D252H/+ show no change in brain to body weight ratio as their brains and bodies are both 96% of wild type at this time point.

Previous studies have found noted loss of muscle bulk in eEF1A2-null mice (31). The muscle to body mass ratio of D252H/+ mice was calculated and the female mice were found to have a significantly reduced ratio ($p=0.029$ two tailed t-test) , whereas male D252H/+ do not ($p=0.84$ two-tailed t test). The muscle weights of D252H/+ female mice were found to be 79% those of wild type littermates, whilst their total body weights were 90% of wild type.

Mutations in *EEF1A2* in humans are associated with hypotonia, or low muscle tone, often associated with reduced muscle strength. In order to establish whether the same effect is seen in mice, juvenile D252H/+ mice of both sexes were tested for grip strength at P22. Whilst a difference in forelimb-only grip strength was only observed in female mice (Figure 4d), both male and female D252H/+ mice were found to have impaired all-limb grip strength compared to wild-type littermates (Figure 4c). Mice tested at 8 weeks were found to have normal grip strength (Figure 4e-f). This is in contrast with mice heterozygous for a deletion mutation in eEF1A2, which have normal motor function as measured by grip strength and rotarod (21).

These findings, along with the impairments in neuroscore and lowered body weight, demonstrate that the three week-old D252H/+ mouse has subtle but measurable and clinically relevant phenotypic features against which therapies could be tested.

<u>D252H/+ mice show a mild motor deficit on the accelerating rotarod but no behavioural abnormalities</u>

The motor coordination and balance of D252H/+ mice was tested using the accelerating rotarod. Adult female D252H/+ mice showed significantly worse performance on the rotarod than wild type littermates (2-way repeated measures ANOVA showed significant effect of genotype: $F(1,14) = 11.55$, $p = 0.0043$) but genotype was not found to have an effect on rotarod ability in male D252H/+ mice.

As many individuals with mutations in *EEF1A2* have been reported to show autistic behaviours, D252H/+ mice were put through a battery of tests designed to reveal signs of anxiety or hyperactivity, differences in sociability, spatial memory, and repetitive behaviours. Due to the motor deficiency seen in female mice when tested on the rotarod, the behavioural test were restricted to male mice. In all behavioural tests performed (figure 5) no differences were seen between D252H/+ and wild-type mice.

Comparison of eEF1A2 missense and null mice to determine whether the D252H mutation results in loss- or gain-of-function

Having compared D252H/+ mice with wild-type littermates to evaluate the D252H mouse as a model for *EEF1A2* mutations in human, we sought to use the line to provide critical information on the mode of action of the mutation itself. We reasoned that comparing mice homozygous for the missense mutation (D252H/D252H) with eEF1A2 homozygous null mice (-/-) on the same genetic background could yield insights into how the mutation changes the function of the eEF1A2 protein at a physiological level. If homozygous missense mice have a more severe phenotype than homozygous knock-out mice, this would indicate that the knocked-in mutation confers a toxic gain-of-function. Such experiments can now be easily performed using CRISPR-Cas9, since engineering a knock-in model will often involve the simultaneous, unintended, production of knock-out founder animals (since non-homologous end joining repair generates deletions). We compared mice homozygous for the D252H mutation of *Eef1a2* (D252H/D252H) with *Eef1a2* -/- mice. These null mice carry a 22bp deletion in exon 3 of *Eef1a2 (figure S7a)* resulting in a premature stop codon predicted to result in nonsense-mediated decay, and were generated as a by-product of a CRISPR knock-in experiment (22); both experiments were conducted using C57BL/6 donors. Mice homozygous for the deletion in exon 3 express a 10-fold reduction in eEF1A2 mRNA compared to wild type (figure 6a) and no detectable eEF1A2 protein using two different antibodies directed against either terminal of eEF1A2 (Figure 6b and S7b). Importantly,

homozygotes on this genetic background show a high number of sudden deaths and spontaneous fatal seizures around 22 days. The weight-loss profiles do not therefore extend to the age at which body weight is significantly different from wild type littermates, as seen in the original eEF1A2-null mouse on a mixed background (31). However, the weight-loss profiles of both the del22.ex3 and wasted mouse lines are comparable (figure S7c).

Comparative phenotyping of D252H/D252H and -/- mice reveals both loss and gain-of-function

D252H/D252H mice, at first sight, appear similar in phenotype to -/- mice, suggestive of a loss of function in the D252H/D252H mice. Weight gain between P14 and P22 is attenuated in both D252H/D252H and -/- mice (figure 6c and d), and both lines show neurological deficits in comparison to wild-type littermates (Figure 6e and f). We examined pathology in the spinal cord, as null mice have no obvious pathology in the brain but show severe neuronal loss in the spinal cord (31). Spinal cords of both -/- and D252H/D252H mice show abnormal pathology when sectioned (Figure S6b), including loss of normal nuclear structure with apparent loss of nuclear membrane leading to neuronal death in anterior horn motor neurons. Sections stained against glial fibrillary acidic protein (GFAP) as a marker of gliosis show increased GFAP expression in both D252H/D252H and -/- spinal cords compared to wild type (supplementary figure S6a and S6b). This neurodegenerative phenotype is consistent with that previously reported in wasted mice, and is consistent with a loss of function in eEF1A2 causing cellular lethality.

The weight gain profile of juvenile mice shows a sex-specific phenotypic difference between missense and null mutant mice. Whilst D252H/D252H females have a weight profile similar to that of -/- females, male D252H/D252H mice not only weigh less than -/- males at 15 days, they essentially fail to gain weight thereafter. There is a significant difference in weight between D252H/D252H and null males at every day from 15 days until mice have to be culled at ~22 days (Figure 6c and d).

Comparison of the D252H/D252H and -/- mice shows that neurological dysfunction in D252H/D252H mice, as measured by neuroscoring (note that the mice die before they are old enough to be tested on the rotarod) worsens progressively from 16-23 days. Importantly, the scores indicate a significantly

more severe neurological phenotype in the D252H/D252H mice than in the -/- mice, in both males and females (Figure 6e and f).

The greater severity of neurological deficit in both sexes and worse weight gain profile in males indicate that mice carrying the D252H mutation on both copies of the *Eef1a2* gene are more severely affected than mice expressing no eEF1A2 at all. The D252H mutation therefore appears to confer a novel toxic property on the eEF1A2 protein.

Discussion

The unusual mutational profile for *EEF1A2* in affected individuals (numerous independent missense changes, but no internal deletions or mutations leading to premature termination) suggests that the mutations causing severe epilepsy and ID may not operate through a simple loss of function mechanism (23). Establishing the functional consequences of mutations in eEF1A2 is not trivial, because unlike fully differentiated neurons and muscle *in vivo*, all cell lines express high levels of the near-identical protein eEF1A1, with the potential to mask any gain or loss of function of eEF1A2. We therefore exploited the power of CRISPR/Cas9 gene editing to recreate both missense and null alleles in mice, and compared the resulting phenotypes. This phenotyping, in conjunction with proteomic analysis, has for the first time shed light on the way in which one of the pathogenic mutations in *EEF1A2* operates.

We first showed, using an unbiased proteomic approach followed by confirmatory coIP, that the D252H mutation inhibits the binding of eEF1A2 to all components of the GTP exchange factor eEF1B complex. This suggested a possible loss of function (see below) but in order to test this, and to generate a mouse preclinical model, we used CRISPR/Cas9 editing to recreate the mutation *in vivo*. This was successful, with 16/27 founders having mutations at the correct locus of which two had clean missense mutations encoding the D252H mutation.

We then generated lines of D252H/+ mice, accurately recapitulating the genotype of affected human individuals. We analysed expression of eEF1A2 in brain and muscle from heterozygous and homozygous mice in order to assess any impact of the mutation on protein stability. Whilst expression at the RNA level was unaltered in the mutants, eEF1A2 showed reduced abundance at the protein level in the brains of heterozygous (80%) and homozygous mice (60%), suggesting some effect of D252H on stability. Surprisingly, this reduction was not seen in muscle, and indeed levels of mutant eEF1A2 in homozygotes are even higher than in controls. The reasons for this are unclear but it is possible that there are differences in post-translational modifications and or higher order complexes in the different tissues and that these differentially influence stability of the mutant protein.

The D252H/+ mice showed no evidence of spontaneous seizures, but this is consistent with the clinical picture for this specific mutation (one child with this mutation has not been diagnosed with epilepsy

and the other had no seizures before the age of 8). The heterozygous missense mice showed no clear behavioural phenotypic abnormalities, including in tests commonly used as surrogates for autistic behaviours (though this is not unprecedented in mouse models of NDD (32, 33)). Spatial memory, as measured by the Y maze, appeared normal although more sophisticated tests might reveal more subtle effects. The heterozygous mice did, however, show consistently reduced body weight and elevated neuroscores at 16-22 days postnatal in comparison with their wild-type littermates. They also had a significant deficit in all four limb grip strength at 22 days. These phenotypic abnormalities are subtle but consistent with neurodevelopmental abnormalities.

We next tested the hypothesis that the D252H variant is a loss of function mutation by comparing the phenotypes of mice with missense and null mutations. Heterozygous D252H/+ animals show subtle but significant differences from their wild-type littermates, including lower body weight (unlike +/- animals), transiently worse neuroscores and reduced grip strength. The homozygous D252H/D252H mice share features of spinal cord neurodegeneration with the homozygous null mice, consistent with previous studies of wasted mice that have a spontaneous null mutation in eEF1A2 (31). These results are suggestive of a loss of function of eEF1A2 in the presence of the D252H mutation (since the expression levels of mutant protein are in excess of those seen in unaffected heterozygous null animals). However, the missense homozygous mice are more severely affected in terms of neurological function and body weight than their age-matched homozygous null counterparts, in spite of a common genetic background. This suggests that the mutation causes toxicity giving rise to an additional gain of function.

The loss of binding of mutant eEF1A2 to the eEF1B complex might be predicted to result in impairment of protein synthesis. However, our attempts to measure protein synthesis in mouse muscle *in vivo* (to avoid the confounding presence of eEF1A1) using SUnSET (34) gave highly variable results, including an apparent signal in the homozygous null mice preventing us from drawing direct conclusions. This technique has recently been noted to give variable results *in vivo* depending on cell type (35). It is hard to judge the functional consequences of failure of eEF1A2 to bind eEF1B on whole organism physiology, and in fact there is evidence that the effects might not be severe. RNAi knockdown in mammalian cells showed that eEF1B subunits are dispensable for function, at least in the short term

(36), and recently an *Eef1b2* knockout mouse was found to be viable (37). No humans with clear null mutations in genes encoding eEF1B subunits have been described, although there are individuals with mutations in eEF1B subunits with neurodevelopmental disorders (23).

In addition to the apparent loss of function of eEF1A2 in the presence of the D252H mutation, the homozygous D252H mice showed significantly more severe growth retardation than the null mice, most notably across the whole time course in males. Both sexes had significantly worse neuroscores than null mice from as early as 16 days. This profile, of a more severe phenotype in missense mice than in nulls, strongly suggests a toxic gain of function of the D252H mutation.

The lower than normal body weight associated with the presence of D252H mutant protein could be a reflection of the relationship between protein synthesis and cell size. However, the homozygous null animals show no difference in body weight in comparison with normal littermates until ~21 days. In terms of the clinical profile of children with missense mutations the picture is inconsistent due to reporting differences, but the case with a D252H mutation described by Nakajima et al was reported to be 2.5 SD for height and -1.2 SD for weight at age 8. Children with mutations in *EEF1A2* have been reported to have hypotonia, and the heterozygous missense mice have grip strength abnormalities at 22 days. These findings in the mice, whilst non-specific, are thus consistent with those in humans. In contrast, there were no behavioural abnormalities detected in the heterozygous mice that would model those seen in affected children.

Ultimately, the severity of any given mutation may depend on a balance between any toxic effects and the effect of the mutation on protein stability- less stable proteins would presumably be less toxic and the resulting phenotype more like a heterozygous null. Phenotypic severity will undoubtedly also depend on the location of mutations on the protein, and changes in binding partners. Further animal models recapitulating different missense mutations will be needed to address the mechanistic impact of each on the function of neurons and muscle.

Finally, although many questions remain about the functional consequences of mutations in eEF1A2 at the molecular level, we have successfully made a line of mice that recapitulate one of the clinically relevant mutations seen in humans. The finding that this missense mutation has important implications

for the design of therapeutic approaches, since it may be necessary to ablate expression of the mutant protein alongside any replacement based treatment. The phenotypic abnormalities we describe have sufficient similarities with those seen in children that the new lines will serve as valuable preclinical models for the testing of therapies.

Materials and methods

Construct generation

The eEF1A2-V5 construct was created by cloning the eEF1A2 cDNA sequence in to the backbone of the pcDNA3.1-V5 vector (Invitrogen). D252H mutation was introduced using the Quik Change II site directed mutagenesis kit (Agilent).

Label-free quantification mass spectrometry

P12-14 SH-SY5Y Cells were transfected using the Turbofect (Thermo Fisher) protocol. 20µg of DNA was transfected into separate T75 flasks. Cell pellets were stored at 80°C, then were resuspended in ice-cold RIPA buffer (150mM sodium chloride, 1% (v/v) NP-40, 0.5% (w/v) sodium deoxycholate, 0.1% (v/v) SDS and 50mM Tris-HCL (pH8) + cOmplete mini protease inhibitor (Roche)), lysed in a Bioruptor for 7 cycles of 30 seconds on and off at 4°C, then spun at 13300xg for 20 minutes. The supernatant was removed and taken for immunoprecipitation.

To isolate eEF1A2-V5 and binding partners, samples were incubated at 4°C for 3 hours with V5 agarose magnetic beads (MBL international), using the KingFisher Duo II robot system. After incubation, the the beads were washed 3 times with 500µl of RIPA buffer and a further 2 times in 500µl TBS. Finally, beads were deposited in trypsin working reagent (42.9mM trypsin protease (Pierce, MS grade), 1mM DTT, 2M UREA, 50mM Tris pH8). Samples were left overnight to digest at 4°C and peptide fragments were collected. Samples were then maintained at -20°C until loading onto the Thermo-Q Orbitrap mass spectrometer for label free quantification (LFQ). LFQ intensities were normalised using two complementary methods: bait normalisation and most-likely ratio normalisation (MLR) (24). Fold-change from the wild-type condition were calculated using both these normalisation strategies.

Co-Immunoprecipitation

$2.8x10^6$ SHSY5Y cells in a T25 flask were transfected with the eEF1A2-V5 construct using Turbofect (Thermo Fisher). After 48 hours cells were trypsinised, spun and pellets lysed in 100ul RIPA buffer.

Cells were sonicated using the Bioruptor (Diagenode) for 7 cycles of 30 seconds on and off. Lysates were spun at 10,000g for 15 minutes and supernatant collected. A bead solution was made by diluting V5 agarose magnetic beads (MBL International) 1 in 10 in RIPA buffer. 10µl of bead solution were added to the cells lysates and samples incubated for 3 hours at 4°C with rotation. Samples were spun in a centrifuge for 2 minutes at 8000 rpm. Using a magnetic Eppendorf rack (Active Motif), beads were isolated and lysate extracted. These lysates were diluted 1:1 in 2X Laemmli buffer and 10% 1M DTT, boiled for 10 minutes at 95°C and stored at -20°C as the 'input' fraction. Beads were washed in 100ul RIPA buffer 3 times and with 300ul TBS twice using volumes described above. 2X Laemmli buffer and RIPA buffer were mixed 1:1 and added to beads. Tubes were incubated for 10 minutes at 95°C, then re-applied to the magnetic rack and supernatant collected. The sample was supplemented with 10% v/v 1M DTT and stored at -20°C as the IP fraction. For western blotting, 15µl of IP fraction and 5µl of input fraction were used with the following antibodies: eEF1Bγ anti-rabbit 1:1000 (Abcam), eEF1Bα anti-rabbit 1:250 (Proteintech), eEF1Bδ anti-rabbit 1:1000 (Proteintech), ValRS anti-rabbit 1:250 (St Johns laboratory) , and V5 anti-mouse 1:1000 (Invitrogen). Secondary antibodies were light chain mouse anti-rabbit HRP 1:1000 (Abcam) and light chain donkey anti-mouse HRP 1:1000 (DAKO). All incubations were 1 hour room temperature unless otherwise specified.

CRISPR/Cas9n gene editing

Guide RNA pairs were designed from target sequence of mouse *Eef1a2* around exon 5 using online tools at http://crispr.mit.edu/. They were synthesised, annealed and cloned into vector px458 from which they were *in vitro* transcribed. The sequences were amplified using universal reverse primer and T7-tagged forward primers. The guide RNA PCR template was used for *in vitro* RNA synthesis using T7 RNA polymerase, and the RNA template was subsequently purified using RNeasy mini kit (Qiagen) purification columns. Cas9 nickase mRNA was procured from Tebu Bioscience. The repair template was designed and synthesised as 200bp PAGE-purified ssODN Ultramer by IDT.

Transgenic mouse generation

Mice were housed in the Biomedical Research Facility (BRF) at the University of Edinburgh. All mice were maintained in accordance with Home Office regulations and all protocols had been approved by the local ethics committee of the University of Edinburgh. All methods were performed in accordance with the relevant guidelines and regulations. Embryo transfer was carried out with short term recovery anaesthesia, and analgesia where needed post-operatively. Mutant mice were closely observed for overall clinical condition and were euthanized where necessary to avoid suffering.

Transgenic mice were made using pronuclear injection of CRISPR reagents into oocytes derived from C57BL/6JCrl mice. The microinjection mix was prepared with components at the following concentrations: gRNAs 25 ng/ul each, Cas9n mRNA at 50 ng/ul and Ultramer ssODN repair template 150 ng/ul. There were 28 live born mice as a result of this procedure; two of which were found to carry the desired point mutation in *Eef1a2* (c.G754C) and became founders of the transgenic mouse lines used in subsequent experiments described here.

Mice that survived weaning were housed in single sex, mixed genotype groups of between 2 and 5 animals. Both male and female mice were characterised, numbers and ages of mice are described for each test. All phenotyping was carried out blind to genotype.

Genotyping

Ear notches were taken at 14 days after birth, DNA extracted and used for PCR genotyping, initially by direct sequencing when identifying founders, then after establishment of D252H colonies by restriction digests of PCR products to detect the presence/absence of the Hin1II restriction site created by the D252H mutation. PCR primers used were 5'-3' AGGCTACCCCTTAGGCAGGT, TGAACAAATGGTAGGTGGGAGG. Animals from the eEF1A2$^{-/-}$ line were genotyped by PCR of the region flanking the 11bp deletion using primers 5'-3' TGAGTTGTGCCTCTACCCTT, ACACCTGGGATGTGCCTGTA, The product of the deletion allele was 186 bp and the WT equivalent was 208 bp. These were resolved by running on an 2% agarose gel.

Protein analysis

Whole brains and hind limb muscles were dissected, frozen on dry ice and stored at -70°C until use. They were homogenised in 10µl/mg tissue 0.32M sucrose containing protease inhibitor (cOmplete Mini, Roche) then centrifuged at 17,000g at 4°C for 30 minutes. The supernatant was removed and mixed with 4x NuPAGE LDS sample buffer and 10x NuPAGE reducing agent, then heated to 70°C for 10 minutes. Lysates were loaded onto NuPAGE 4-12% bis-tris gels and run at 200V in NuPAGE MOPS SDS, before being transferred onto PVDF membrane (Amersham Hybond) in NuPAGE transfer buffer. Total protein on the blots was visualised using Revert solution (LI-COR). Blots were then blocked in Odyssey blocking buffer (LI-COR) for 1 hour, incubated either 1:5000 in an antibody to eEF1A2 (custom made by Proteintech) or 1:2000 in rabbit anti-eEF1A2 (ab82912 Abcam) for 1 hour, washed in TBS buffer containing 0.01% tween-20 for 3x 15 minutes, then incubated in IRdye 800CW anti-rabbit (LI-COR) secondary antibody for 1 hour. After another set of washes, images were taken using the Odyssey CLx (LI-COR) and analysed on Image Studio Lite Version 5.2. eEF1A2 levels were measured by normalising each eEF1A2 band to total protein levels within the lane. All Western blots were performed in triplicate. Differences in the eEF1A2 expression of D252H/+ and D252H/D252H mouse tissues were expressed as fold-change difference from the mean wild type signal.

RNA analysis

RNA from brain was extracted using the QIAGEN RNeasy mini kit and DNase digested using the QIAGEN RNase-Free DNase Set. cDNA was then synthesized using the Agilent Technologies AffinityScript Multi Temperature cDNA Synthesis Kit. Quantitative RT-PCR (qPCR) was performed on the cDNA using primers for eEF1A2 exon 2-4 (5′ GCCACGATCAGCACTGCG and 5′ CAAGCGGACCATCGAGAAGT), eEF1A2 exon 3-4 (5'ATATGATTACAGGCACATCCCAG and 5'GTGCGTGTTCCCGGGTTT), Actin (5' TCCATCATGAAGTGTGACGT and 5' GAGCAATGATCTTGATCTTCA) and GAPDH (5'GGAAGGGCTCATGACCACA and 5'CCGTTCAGCTCTGGGATGAC) were selected as suitable reference genes after analysis with a geNorm 6 gene mouse kit (PrimerDesign). Brilliant II SYBR Green QPCR master mix (Agilent) was used to make the reaction mix. cDNA was diluted 1:10 and 4µl added to each reaction. Sample were

run in triplicate in a LightCycler HT7900 (Roche) and quantity means were calculated using Ct values along with the slope and the Y-intercept from the standard curve for each gene.

Grip strength

Limb muscle strength was measured at P22 and 8 weeks of age using a grip strength meter (Bioseb). Grip strength from all four limbs or front limbs only was measured in triplicate with a 1-minute break in between each test to allow the mouse to rest. For each test the mouse was held by the base of the tail and lowered onto the grid until it gripped with either the front paws or all four paws, and then pulled horizontally away from the grid. The maximum force (Newton, N) was recorded.

Neuroscore

To assess the neurological phenotype of mutant mice four tests adapted from Guyenet et al, (25) were applied to each animal from P16 to P22, and at 8 weeks of age: Ledge walking, hindlimb clasping, observation of gait, degree of kyphosis. The response of the mice to each test was scored between 0 and 3, and the four test scores combined to give an overall 'neuroscore' between 0 and 12, where a higher number indicates a more severe neurological phenotype. The protocol and scoring criteria for each test are found in supplementary methods 1.

Rotarod

Mice were tested for balance or motor deficiencies by measuring how long they could stay on an accelerating rotating beam (Bioseb). Mice were trained on day 1 of the experiment by placing them on a rotarod moving at a constant speed of 4rpm. Mice were replaced back on the rotarod if they fell off until they were able to stay on for at least a minute without dropping. At this point the rotarod was accelerated from 4 to 40rpm over 2 minutes. When mice fell off in this phase they were not replaced on the beam. Mice were rested for 30 minutes and then tested as follows: mice were placed, facing away from the investigator, on a beam rotating at 4rpm. The rotarod was then accelerated to 40rpm over a period of 2 minutes and the time taken for mouse to drop recorded, up to a maximum time of 3 minutes. Mice were tested three times per day with a 30 minute rest period in between. Each animal was tested on three days with a day of rest in between each test day.

Microcephaly

For each sex, five +/+ mice and five D252H/+ mice were euthanised at P60. Brains were dissected and post-fixed in 4% PFA for 24 hours before being mounted in paraffin. 10 μM coronal sections were taken and stained using H&E before being imaged at 20x magnification using a Nanozoomer slide scanner (Hamamatsu). Using the Allen mouse brain atlas, brain sections corresponding to Bregma ± 0 mm and Bregma -1.6 mm were selected for analysis. Annotation and measurement of different brain regions was performed using the Ndp.view2 software (Hamamatsu). Brain measurements were statistically analysed using repeated measures one-way ANOVA, with each D252H/+ mouse matched with one same-sex +/+ littermate.

Mouse behavioural testing

Male mice were tested between 2 and 4 months of age, in the order described below. Light levels in all tests involving arenas were set to 100 lux. The standard cage described here is 332x150x130mm in size. Where appropriate, cages were cleaned between trials with 1% conficlean.

Marble burying: 20 marbles were placed in 4 rows of 5 in a standard cage containing 5cm of fresh bedding. The mouse was placed in the cage and allowed to explore for 30 minutes. Videos were recorded to score number of marbles 2/3 buried or more.

Digging: Fresh bedding was added to a standard cage and the test mouse allowed to explore for 3 minutes. Latency to onset of digging, number of digging bouts and duration of digging bouts were measured by the observer..

Open field: Mice were placed in the centre of a 50x50cm white perspex arena with 38cm high walls, allowed to explore for 5 minutes and recorded from above. Videos were analysed using Any Maze software to determine total distance travelled by the mouse, time spent freezing and time spent in the central area (this was defined as a 30cm x30cm area in the centre of the arena).

Y-maze: The Y-maze was made of clear perspex with three 40x10cm arms set at 120° to one another, with 16cm-high walls. The floor of the maze was covered with fresh bedding and a handful of bedding from each cage of the test mice. The test mouse was placed in one arm of the maze facing the end wall

and allowed to explore two arms for 5 minutes. After a 15-minute inter-trial interval (ITI), the gate closing the third arm was removed and mouse placed back in the same start arm and allowed to explore the maze for 2 minutes. Bedding was mixed and gate and maze walls cleaned with 1% conficlean between trials. Videos were scored for time spent in each arm during test phase.

Stranger mouse exposure: The stranger mouse experiment was carried out in the Y-maze arena. The start arm was closed using a gate and two wire mesh gates were placed in each arm to form 10cm-long enclosures halfway along the second and third arms. The test mouse was habituated to the y-maze for 10 minutes. It was then removed and a novel adult male mouse unrelated to the test mouse placed in one of the 10cm-long enclosures. The test mouse was returned to the start arm of the maze and allowed to explore for 10 minutes. The test mouse was then removed again and a second novel mouse placed in the other enclosure in the previously unoccupied arm. The test mouse was then returned to the start arm and allowed to explore for another 10 minutes. The positions of novel mouse 1 was counterbalanced between mice. Exploration was defined as the test mouse being in close proximity to and facing the stranger mouse/gate**.**

Nest Building: Fresh mouse bedding was added to a clean cage and a 5cm x 5cm square of nest material weighed and placed in the centre. The test mouse was placed in one corner of the cage and then left overnight. The nestlet was then removed from the cage, allowed to dry overnight and scored according to the scale devised by Deacon(26).

Pathology

P22 mice were euthanised and spinal columns were dissected and fixed in formalin for 24 hours then decalcified for 3 weeks in 10% EDTA (pH7.4; changed weekly), and then placed in formalin for 24 hours. Sections were stained with haematoxylin and eosin by Division of Pathology, University of Edinburgh. Other sections were immunostained for GFAP by taking sections to water, treating with proteinase K for 10 minutes, washing in water, treating with 3% hydrogen peroxide for 10 minutes and then rewashing in water followed by PBS. Sections were blocked for 10 minutes in goat serum, 1:5 in PBS, then incubated in 1:500 GFAP anti-rabbit antibody (Z0334 Dako) overnight, biotinylated

secondary goat anti-rabbit 1:500 for 30 minutes, Streptavidin ABS for 30 minutes and DAB for 2 minutes, with 5 minute PBS washes between each step. Slides were counterstained with haematoxylin.

Protein modelling

A BLAST alignment (27) confirmed the human eEF1A2 sequence [residues 1-463; NCBI reference sequence: NP_001949.1] had a sequence identity of 100% (E value of 0.0) against the *Oryctolagus cuniculus* eEF1A2 structure available in the Protein Data Bank. The human eEF1A2 protein structure was then modelled through the program I-TASSER (Iterative Threading Assembly Refinement) (28) which utilises meta-threading, replica-exchange Monte Carlo simulations and identification of the lowest free energy states via SPICKER. The resulting .pdb file was then loaded into PyMOL (The PyMOL Molecular Graphics System, Version 2.0 Schrödinger, LLC) and the mutagenesis tool employed to create the D252H mutation, with a rotamer of the lowest free energy and atomic overlap.

Statistics All statistics were performed using GraphPad Prism V8 or in R. T-tests were used in cases where two datasets were compared, except where data were not normally distributed, in which case the Mann-Whitney test was used. Time courses were analysed with repeated measures ANOVA (Figures 3a and 3d, 4g, 4h) or linear mixed models in the cases where some measurements were missing (Figures 3b, 3e, 6b and 6c). LMMs included fixed effects of genotype and age, with animal ID as a random effect, fits were performed using the "lme4" R package (29), and post-hoc tests were performed using the "lsmeans" R package (30). Neuroscore time-courses (a non-continuous measure) were analysed with t-tests of animal averages.

Acknowledgements

We thank the staff of the Bioresearch and Veterinary Services Facilities for expert technical assistance, in particular Emma Allan for microinjections and Hemant Bengani for help with generating the CRISPR reagents. We are very grateful to the staff of the Mass Spectrometry Core at the IGMM, in particular Alex von Kriegsheim and Jimi Wills for their help and advice. Thank you to Bob Hill, Andrew Wood and Ian Jackson for their helpful review of this manuscript.

We are grateful to the the Patrick Wild Centre, the Simons Initiative for the Developing Brain and the R.S. Macdonald Trust for funding. JEH was supported by a BBSRC studentship, FM was supported by an MRC studentship and GFM was supported by a studentship from Medical Research Scotland.

References

1 Soares, D.C., Barlow, P.N., Newbery, H.J., Porteous, D.J. and Abbott, C.M. (2009) Structural models of human eEF1A1 and eEF1A2 reveal two distinct surface clusters of sequence variation and potential differences in phosphorylation. *PLoS One*, **4**, e6315.

2 Nickels, K.C., Zaccariello, M.J., Hamiwka, L.D. and Wirrell, E.C. (2016) Cognitive and neurodevelopmental comorbidities in paediatric epilepsy. *Nat Rev Neurol*, **12**, 465-476.

3 Griffin, A., Hamling, K.R., Hong, S., Anvar, M., Lee, L.P. and Baraban, S.C. (2018) Preclinical Animal Models for Dravet Syndrome: Seizure Phenotypes, Comorbidities and Drug Screening. *Front Pharmacol*, **9**, 573.

4 de Ligt, J., Willemsen, M.H., van Bon, B.W., Kleefstra, T., Yntema, H.G., Kroes, T., Vulto-van Silfhout, A.T., Koolen, D.A., de Vries, P., Gilissen, C. *et al.* (2012) Diagnostic exome sequencing in persons with severe intellectual disability. *N Engl J Med*, **367**, 1921-1929.

5 Veeramah, K.R., Johnstone, L., Karafet, T.M., Wolf, D., Sprissler, R., Salogiannis, J., Barth-Maron, A., Greenberg, M.E., Stuhlmann, T., Weinert, S. *et al.* (2013) Exome sequencing reveals new causal mutations in children with epileptic encephalopathies. *Epilepsia*, **54**, 1270-1281.

6 Nakajima, J., Okamoto, N., Tohyama, J., Kato, M., Arai, H., Funahashi, O., Tsurusaki, Y., Nakashima, M., Kawashima, H., Saitsu, H. *et al.* (2015) De novo EEF1A2 mutations in patients with characteristic facial features, intellectual disability, autistic behaviors and epilepsy. *Clin Genet*, **87**, 356-361.

7 Lam, W.W., Millichap, J.J., Soares, D.C., Chin, R., McLellan, A., FitzPatrick, D.R., Elmslie, F., Lees, M.M., Schaefer, G.B., study, D.D.D. *et al.* (2016) Novel de novo EEF1A2 missense mutations causing epilepsy and intellectual disability. *Mol Genet Genomic Med*, **4**, 465-474.

8 Inui, T., Kobayashi, S., Ashikari, Y., Sato, R., Endo, W., Uematsu, M., Oba, H., Saitsu, H., Matsumoto, N., Kure, S. *et al.* (2016) Two cases of early-onset myoclonic seizures with continuous parietal delta activity caused by EEF1A2 mutations. *Brain & development*, **38**, 520-524.

9 Lopes, F., Barbosa, M., Ameur, A., Soares, G., de Sa, J., Dias, A.I., Oliveira, G., Cabral, P., Temudo, T., Calado, E. *et al.* (2016) Identification of novel genetic causes of Rett syndrome-like phenotypes. *J Med Genet*, **53**, 190-199.

10 de Kovel, C.G., Brilstra, E.H., van Kempen, M.J., Van't Slot, R., Nijman, I.J., Afawi, Z., De Jonghe, P., Djemie, T., Guerrini, R., Hardies, K. *et al.* (2016) Targeted sequencing of 351 candidate genes for epileptic encephalopathy in a large cohort of patients. *Mol Genet Genomic Med*, **4**, 568-580.

11 Cao, S., Smith, L.L., Padilla-Lopez, S.R., Guida, B.S., Blume, E., Shi, J., Morton, S.U., Brownstein, C.A., Beggs, A.H., Kruer, M.C. *et al.* (2017) Homozygous EEF1A2 mutation causes dilated cardiomyopathy, failure to thrive, global developmental delay, epilepsy and early death. *Hum Mol Genet*, **26**, 3545-3552.

12 Lance, E.I., Kronenbuerger, M., Cohen, J.S., Furmanski, O., Singer, H.S. and Fatemi, A. (2018) Successful treatment of choreo-athetotic movements in a patient with an EEF1A2 gene variant. *SAGE Open Med Case Rep*, **6**, 2050313X18807622.

13 Epi25 Collaborative. Electronic address, s.b.u.e.a. and Epi, C. (2019) Ultra-Rare Genetic Variation in the Epilepsies: A Whole-Exome Sequencing Study of 17,606 Individuals. *American journal of human genetics*.

14 Mefford, H.C., Cook, J. and Gospe Jr, S.M. Epilepsy due to 20q13.33 subtelomere deletion masquerading as pyridoxine-dependent epilepsy. *Am J Med Genet A*.

15 Okumura, A., Atsushi, I., Shimojima, K., Kurahashi, H., Yoshitomi, S., lmai, K., Imamura, M., Seki, Y., Toshiaki Shimizu, T., Hirose, S. *et al.* (2015) Phenotypes of children with 20q13.3 microdeletion affecting KCNQ2 and CHRNA4. *Epileptic Disord*, **17**, 165-171.

16 Sasikumar, A.N., Perez, W.B. and Kinzy, T.G. (2012) The many roles of the eukaryotic elongation factor 1 complex. *Wiley interdisciplinary reviews. RNA*, **3**, 543-555.

17 Lee, S., Francoeur, A.M., Liu, S. and Wang, E. (1992) Tissue-specific expression in mammalian brain, heart, and muscle of S1, a member of the elongation factor-1 alpha gene family. *J Biol Chem*, **267**, 24064-24068.

18 Khalyfa, A., Bourbeau, D., Chen, E., Petroulakis, E., Pan, J., Xu, S. and Wang, E. (2001) Characterization of elongation factor-1A (eEF1A-1) and eEF1A-2/S1 protein expression in normal and wasted mice. *J Biol Chem*, **276**, 22915-22922.

19 Colantuoni, C., Lipska, B.K., Ye, T., Hyde, T.M., Tao, R., Leek, J.T., Colantuoni, E.A., Elkahloun, A.G., Herman, M.M., Weinberger, D.R. *et al.* (2011) Temporal dynamics and genetic control of transcription in the human prefrontal cortex. *Nature*, **478**, 519-523.

20 Chambers, D.M., Peters, J. and Abbott, C.M. (1998) The lethal mutation of the mouse wasted (wst) is a deletion that abolishes expression of a tissue-specific isoform of translation elongation factor 1alpha, encoded by the Eef1a2 gene. *Proc Natl Acad Sci U S A*, **95**, 4463-4468.

21 Griffiths, L.A., Doig, J., Churchhouse, A.M., Davies, F.C., Squires, C.E., Newbery, H.J. and Abbott, C.M. (2012) Haploinsufficiency for translation elongation factor eEF1A2 in aged mouse muscle and neurons is compatible with normal function. *PLoS One*, **7**, e41917.

22 Davies, F.C., Hope, J.E., McLachlan, F., Nunez, F., Doig, J., Bengani, H., Smith, C. and Abbott, C.M. (2017) Biallelic mutations in the gene encoding eEF1A2 cause seizures and sudden death in F0 mice. *Sci Rep*, **7**, 46019.

23 McLachlan, F., Sires, A.M. and Abbott, C.M. (2019) The role of translation elongation factor eEF1 subunits in neurodevelopmental disorders. *Hum Mutat*, **40**, 131-141.

24 Lambert, J.P., Ivosev, G., Couzens, A.L., Larsen, B., Taipale, M., Lin, Z.Y., Zhong, Q., Lindquist, S., Vidal, M., Aebersold, R. *et al.* (2013) Mapping differential interactomes by affinity purification coupled with data-independent mass spectrometry acquisition. *Nat Methods*, **10**, 1239-1245.

25 Guyenet, S.J., Furrer, S.A., Damian, V.M., Baughan, T.D., La Spada, A.R. and Garden, G.A. (2010) A simple composite phenotype scoring system for evaluating mouse models of cerebellar ataxia. *J Vis Exp*.

26 Deacon, R.M. (2006) Assessing nest building in mice. *Nature protocols*, **1**, 1117-1119.

27 Altschul, S.F., Madden, T.L., Schaffer, A.A., Zhang, J., Zhang, Z., Miller, W. and Lipman, D.J. (1997) Gapped BLAST and PSI-BLAST: a new generation of protein database search programs. *Nucleic Acids Res*, **25**, 3389-3402.

28 Yang, J., Yan, R., Roy, A., Xu, D., Poisson, J. and Zhang, Y. (2015) The I-TASSER Suite: protein structure and function prediction. *Nat Methods*, **12**, 7-8.

29 Bates, D., Machler, M., Bolker, B.M. and Walker, S.C. (2015) Fitting Linear Mixed-Effects Models Using lme4. *J Stat Softw*, **67**, 1-48.

30 Lenth, R.V. (2016) Least-Squares Means: The R Package lsmeans. *J Stat Softw*, **69**, 1-33.

31 Newbery, H.J., Gillingwater, T.H., Dharmasaroja, P., Peters, J., Wharton, S.B., Thomson, D., Ribchester, R.R. and Abbott, C.M. (2005) Progressive loss of motor neuron function in wasted mice: effects of a spontaneous null mutation in the gene for the eEF1 A2 translation factor. *J Neuropathol Exp Neurol*, **64**, 295-303.

32 Gompers, A.L., Su-Feher, L., Ellegood, J., Copping, N.A., Riyadh, M.A., Stradleigh, T.W., Pride, M.C., Schaffler, M.D., Wade, A.A., Catta-Preta, R. *et al.* (2017) Germline Chd8 haploinsufficiency alters brain development in mouse. *Nature neuroscience*, **20**, 1062-1073.

33 Chadman, K.K., Gong, S., Scattoni, M.L., Boltuck, S.E., Gandhy, S.U., Heintz, N. and Crawley, J.N. (2008) Minimal aberrant behavioral phenotypes of neuroligin-3 R451C knockin mice. *Autism Res*, **1**, 147-158.

34 Schmidt, E.K., Clavarino, G., Ceppi, M. and Pierre, P. (2009) SUnSET, a nonradioactive method to monitor protein synthesis. *Nat Methods*, **6**, 275-277.

35 Hidalgo San Jose, L. and Signer, R.A.J. (2019) Cell-type-specific quantification of protein synthesis in vivo. *Nature protocols*, **14**, 441-460.

36 Cao, Y., Portela, M., Janikiewicz, J., Doig, J. and Abbott, C.M. (2014) Characterisation of translation elongation factor eEF1B subunit expression in mammalian cells and tissues and co-localisation with eEF1A2. *PLoS One*, **9**, e114117.

37 Dickinson, M.E., Flenniken, A.M., Ji, X., Teboul, L., Wong, M.D., White, J.K., Meehan, T.F., Weninger, W.J., Westerberg, H., Adissu, H. *et al.* (2016) High-throughput discovery of novel developmental phenotypes. *Nature*, **537**, 508-514.

Figure 1 The location of the D252H mutation in human eEF1A2 and effect on binding partners

(a) Location of missense mutation D252H and known binding sites mapped onto 3-D model of yeast eEF1A using PyMOL. The equivalent locations of the eEF1Bα (yellow) and the GTP/GDP (blue) binding sites are also highlighted as in (1). **(b)** Changes in the eEF1A2-interactome due to the D252H mutation after affinity-purified mass-spectrometry of cell lysates transfected with either wild type or mutated (D252H) eEF1A2-V5. Volcano plot shows Log2 fold change plotted against the corresponding -log10 p-value. P-values were calculated using one t-test per protein with a 1% FDR correction for multiple testing. Proteins were defined as significant (green) when there was a log2 fold change greater than 1 and $p < 0.05$. Non-significant proteins were identified in blue. **(c)** Co-immunoprecipitation experiments in SH-SY5Y cells carried out in duplicate transfections. eEF1A2-V5 was isolated using the V5 tag and western blot used to probe for top four proteins identified in (b).

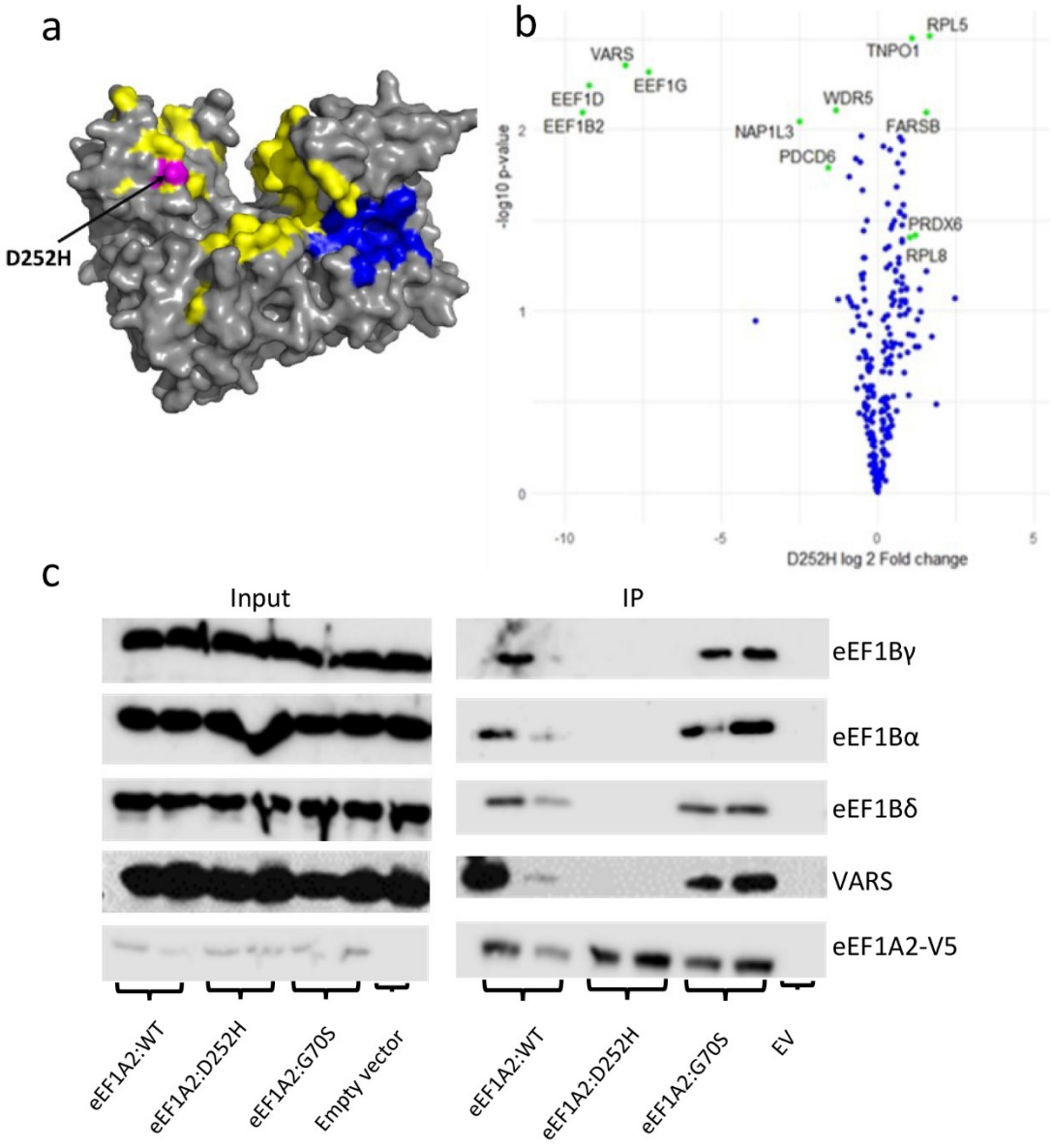
a
D252H
b
RPL5
TNPO1
VARS
EEF1G
EEF1D
EEF1B2
WDR5
NAP1L3
FARSB
PDCD6
PRDX6
RPL8
-log10 p-value
2
1
0
-10
-5
0
5
D252H log 2 Fold change
c
Input
IP
eEF1Bγ
eEF1Bα
eEF1Bδ
VARS
eEF1A2-V5
eEF1A2:WT
eEF1A2:D252H
eEF1A2:G70S
Empty vector
eEF1A2:WT
eEF1A2:D252H
eEF1A2:G70S
EV

Figure 2 A mouse line carrying the D252H mutation was engineered using CRISPR. (a) The gRNA sequences used are blue, bases mutated in the repair template to alter the PAM sites are highlighted green. The site of the desired mutation 754G>C (D252H) is highlighted yellow. **(b)** Mice born after microinjection of CRISPR components according to genotype. **(c)** Sequencing chromatogram of DNA isolated from one of the two founders. The two overlaid peaks at the position marked 'S' show the sequenced mouse to be heterozygous for the 754G>C mutation **(d)** qPCR analysis of RNA taken from the brains of 3 D252H/+ and 3 D252H/D252H mice using primers within eEF1A2 shows no significant difference between genotypes (1-way ANOVA F(2,6,) = 0.32 P= 0.7) **(e)** Representative western blot of muscle lysates from wild type and D252H mutant P22 mice showing eEF1A2 abundance normalised to total protein levels, quantified in **(f)** p=0.0006 t(16)=4.2 unpaired two-tailed t test. **(g)** Representative western blot of brain lysates from wild type and D252H mutant mice, quantified in **(h)** p=0.0002 t(18)=4.5 unpaired two-tailed t test. Each dot in (f) and (h) represents single mouse and is the mean of three technical repeats

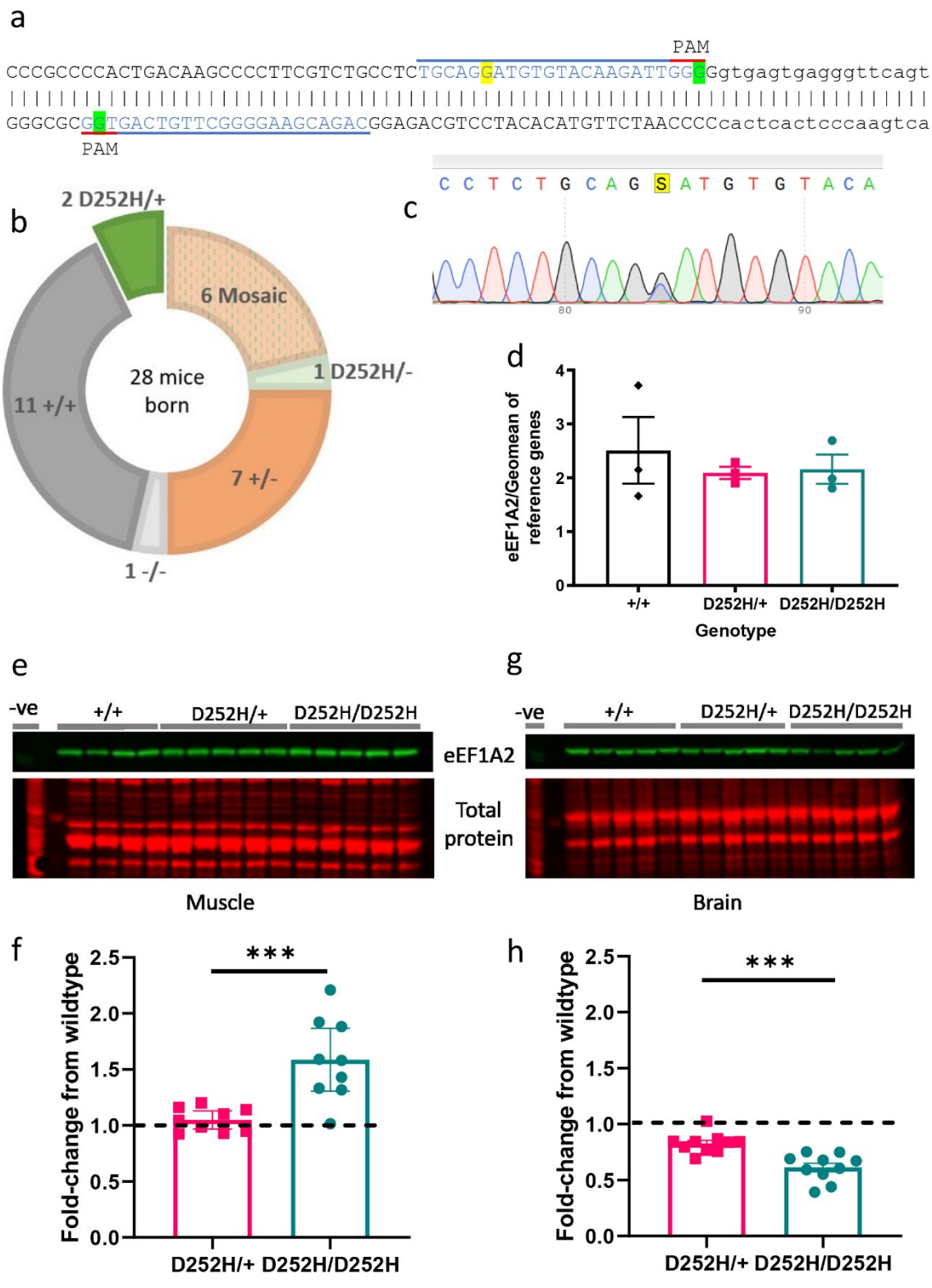
a
PAM
CCCGCCCCACTGACAAGCCCCTTCGTCTGCCTCTGCAGGATGTGTACAAGATTGGCGgtgagtgagggttcagt
GGGCGCGCTGACTGTTCGGGGAAGCAGACGGAGACGTCCTACACATGTTCTAACCCCcactcactcccaagtca
PAM
b
2 D252H/+
6 Mosaic
1 D252H/-
28 mice born
11 +/+
7 +/-
1 -/-
c
C C T C T G C A G S A T G T G T A C A
80
90
d
eEF1A2/Geomean of reference genes
0
1
2
3
4
+/+
D252H/+
D252H/D252H
Genotype
e
-ve
+/+
D252H/+
D252H/D252H
eEF1A2
Total protein
Muscle
g
-ve
+/+
D252H/+
D252H/D252H
Brain
f
Fold-change from wildtype
0.0
0.5
1.0
1.5
2.0
2.5
***
D252H/+
D252H/D252H
h
Fold-change from wildtype
0.0
0.5
1.0
1.5
2.0
2.5
***
D252H/+
D252H/D252H

Figure 3 Body weights and neuroscores of D252H/+ mice and wild type littermates. (a) male and **(d)** female D252H/+ and wild type littermate mouse weights between 3 and 13 days post birth, n=12. Repeated measures ANOVA shows no significant difference between genotypes. **(b)** Male and **(e)** female body weights between 14 and 22 days post birth n>12 (male D252H/+ vs +/+, p=0.0001; female D252H/+ vs +/+, p= 0.0018; linear mixed model) **(c)** male and **(f)** female body weights of adult D252H/+ and +/+ littermates at 8 weeks post birth. Male (p=0.009 t(17)=2.9) and female (p=0.001 t(21)=4.3) D252H/+ mice weigh significantly less than +/+ littermates, two-tailed unpaired t test. **(g)** Male and **(h)** female neuroscore between 16 and 23 days post birth (male D252H/+ vs +/+, t(38.3)=3.75, p=0.0006; female D252H/+ vs +/+, t(62.0)=4.08, p= 0.0001; unpaired two-tailed t-test, animal means). **(i)** Male and female adult neuroscores show no significant difference between D252H/+ and wild type littermates in an unpaired two-tailed t-test (male female p=0.27 t(16)=1.1) .

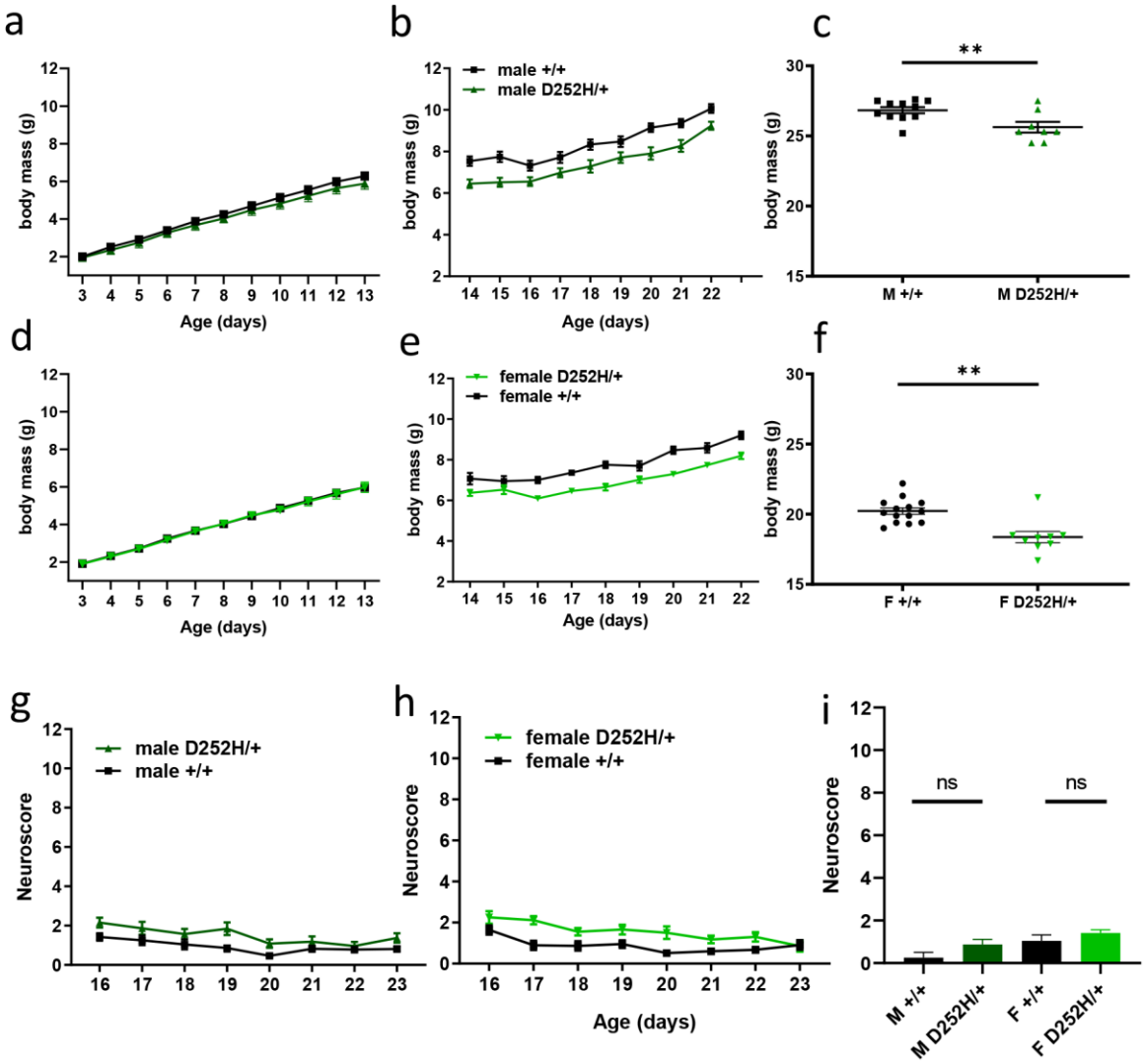
a
b
c
d
e
f
g
h
i
body mass (g)
Age (days)
male +/+
male D252H/+
female +/+
female D252H/+
M +/+
M D252H/+
F +/+
F D252H/+
**
Neuroscore
ns

Figure 4: Body measurements, grip strength and rotarod performance of D252H/+ mice. **(a)** Brain and **(b)** muscle weights of P22 D252H/+ and wild type littermates expressed as ratio to body weight. Welch's t-test shows female D252H/+ have a higher brain to body weight ratio than wild type littermates ($p=0.009$ $T(16)=2.9$)) and a lower muscle to body weight ratio ($p=0.002$ $T(13)$-3.7). **(c)** All-limb and **(d)** front-limb grip strengths of P22 D252H/+ mice and wild type littermates. Two-tailed unpaired t tests show males and females have impaired all-limb grip strength at P22 (males $p<0.0001$ $t(26)=4.6$, females $p=0.0002$ $t(228)=4.3$) and females also show an impaired front-limb grip strength ($p=0.0056$ $t(28)=3.0$). **(e)** all-limb and **(f)** front-limb grip strengths at 8 weeks of age show no significant difference from wild type using an unpaired t-test. **(g)** Female and **(h)** male rotarod experiments (n=8 for each sex/genotype) show female D252H/+ have an impaired ability on the rotarod compared to wild type littermates (2-way repeated measures ANOVA showed significant effect of genotype for females: $F(1,14) = 11.55$, $p=0.0043$, but not males $F(1,16)=0.88$ $P=0.36$).

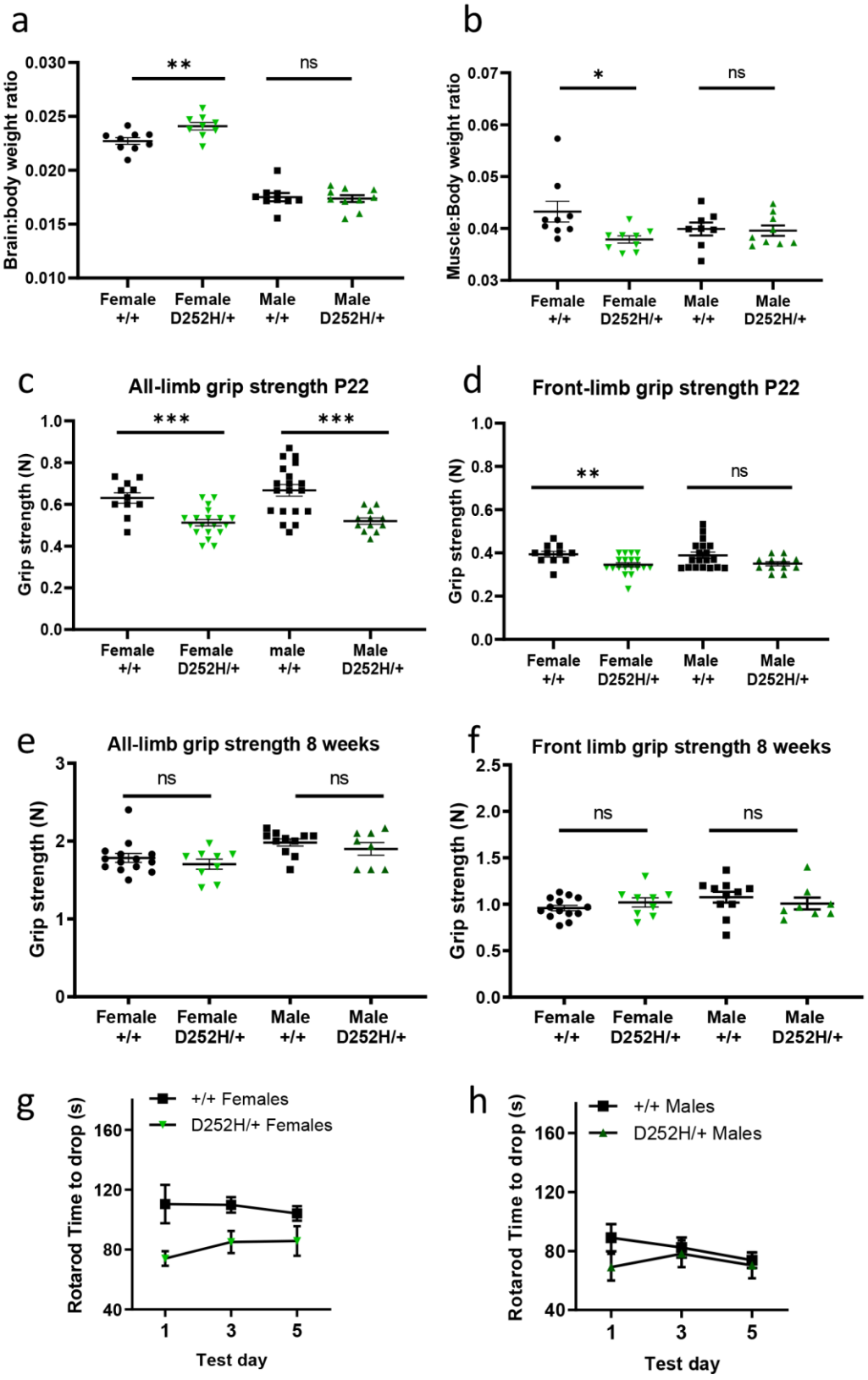
a
Brain:body weight ratio
0.030
0.025
0.020
0.015
0.010
**
ns
Female +/+
Female D252H/+
Male +/+
Male D252H/+
b
Muscle:Body weight ratio
0.07
0.06
0.05
0.04
0.03
*
ns
Female +/+
Female D252H/+
Male +/+
Male D252H/+
c
All-limb grip strength P22
Grip strength (N)
1.0
0.8
0.6
0.4
0.2
0.0
***
***
Female +/+
Female D252H/+
male +/+
Male D252H/+
d
Front-limb grip strength P22
Grip strength (N)
1.0
0.8
0.6
0.4
0.2
0.0
**
ns
Female +/+
Female D252H/+
Male +/+
Male D252H/+
e
All-limb grip strength 8 weeks
Grip strength (N)
3
2
1
0
ns
ns
Female +/+
Female D252H/+
Male +/+
Male D252H/+
f
Front limb grip strength 8 weeks
Grip strength (N)
2.5
2.0
1.5
1.0
0.5
0.0
ns
ns
Female +/+
Female D252H/+
Male +/+
Male D252H/+
g
+/+ Females
D252H/+ Females
Rotarod Time to drop (s)
160
120
80
40
1
3
5
Test day
h
+/+ Males
D252H/+ Males
Rotarod Time to drop (s)
160
120
80
40
1
3
5
Test day

Figure 5 Behavioural phenotyping of adult D252H/+ mice. **(a)** repetitive behaviour measured by marble burying test shows no significant difference in number of marbles buried between D252H/+ and +/+ littermates. (unpaired t-test). See also supplementary figures S5a-e for other repetitive behaviour tests. **(b**) open field test measuring anxiety and hyperactivity. No significant difference is seen between genotypes in the time mice spend in the centre of the maze (unpaired t-test). See also supplementary figures S5f-g. **(c**) Y-maze test measuring spatial memory. D252H/+ mice show normal preference for social novelty as defined here by a novel:familiar ratio not equal to zero (One sample-Wilcoxon test +/+ p= 0.002 W=55, D252H/+ p=0.002 W=55), but there is no significant difference in novel:familiar ratio between genotypes (Mann-Whitney two-tailed test p=0.19 U=32) **(d)** Stranger mouse test show D252H/+ mice have normal sociability, preferentially exploring a y-maze arm containing a stranger mouse over an empty arm of the y-maze. (One sample-Wilcoxon test +/+ p= 0.001 W=66, D252H/+ p=0.002 W=55) with no significant difference between genotypes (Mann-Whitney two-tailed test p=0.6 U=47) See also supplementary figures S5.

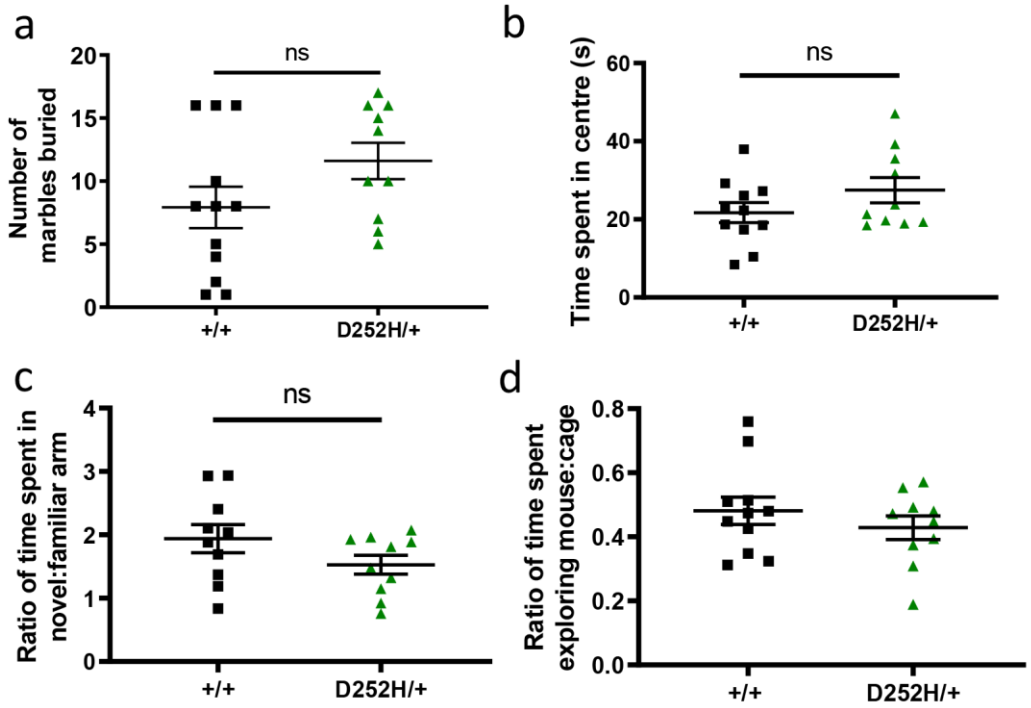

Figure 6 Comparison of homozygous D252H/D252H mice with the eEF1A2 knockout (-/-) mouse **(a)** qPCR showing the mRNA levels of eEF1A2 in -/- brain, measured using two primer sets which amplify a region 3' of the deletion site (exon 3-4) and a region spanning the deletion site (exon2-4) respectively. **(b)** Western blot showing that the eEF1A2 knockout mouse does not express eEF1A2 protein in brain. **(c)** Male and **(d)** female body weights of D252H/D252H, -/- and wild type littermate mice between 14 and 22 days of age (male D252H/D252H vs +/+, $p < 0.0001$; male -/- vs +/+, $p=0.267$; male D252H/D252H vs -/-, $p = 0.0005$; female D252H/D252H vs +/+, $p < 0.0001$; female -/- vs +/+, $p=0.011$; female D252H/D252H vs -/-, $p=0.5188$; linear mixed models) **(e)** Male and **(f)** female neuroscores of D252H/D252H, -/- and wild type littermate mice between 16 and 23 days of age (male D252H/D252H vs +/+, $p < 0.0001$; male -/- vs +/+, $p < 0.0001$; male D252H/D252H vs -/-, $p < 0.0001$; female D252H/D252H vs +/+, $p < 0.0001$; female -/- vs +/+, $p < 0.0001$; female D252H/D252H vs -/-, $p < 0.0001$; 1-way ANOVA with post-hoc Tukey's test, animal means).

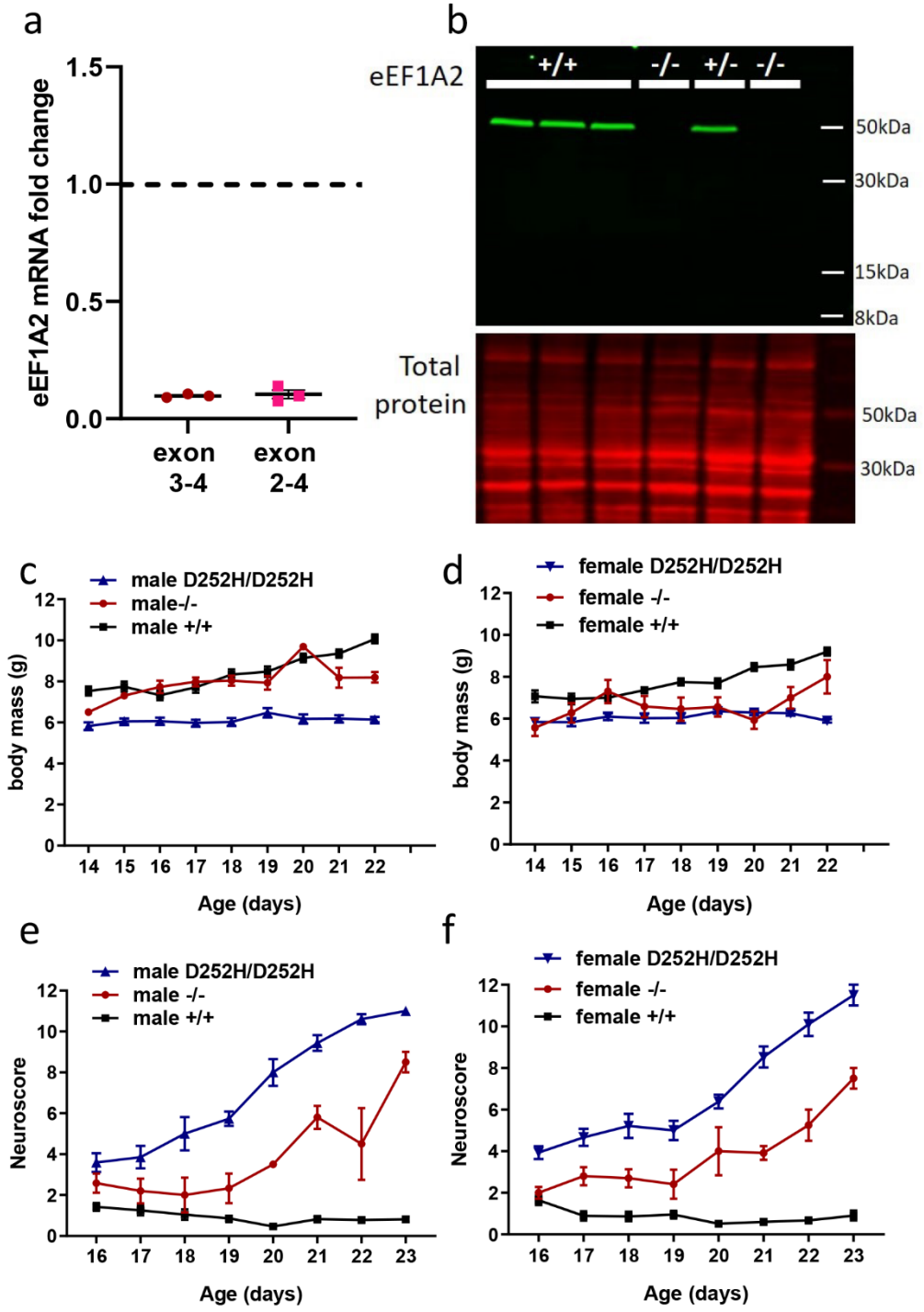
a
eEF1A2 mRNA fold change
1.5
1.0
0.5
0.0
exon 3-4
exon 2-4
b
eEF1A2
+/+
-/-
+/-
-/-
50kDa
30kDa
15kDa
8kDa
Total protein
50kDa
30kDa
c
male D252H/D252H
male-/-
male +/+
body mass (g)
Age (days)
d
female D252H/D252H
female -/-
female +/+
body mass (g)
Age (days)
e
male D252H/D252H
male -/-
male +/+
Neuroscore
Age (days)
f
female D252H/D252H
female -/-
female +/+
Neuroscore
Age (days)

Supplementary Figure S1 Changes in the eEF1A2-interactome due to the D252H mutation after affinity-purified mass-spectrometry of cell lysates transfected with either wildtype or mutated (D252H) eEF1A2-V5. List of proteins with greater than 0.5 $\log_2$ fold change between wildtype and mutant conditions, listing both bait-normalised and MLR-normalised data for each gene. Genes listed in order of largest fold-change to smallest.

	Fold change (Log2)	
Gene name	Bait normalised	MLR normalised
EEF1B2	-8.14295	-9.43204
EEF1D	-8.01752	-9.21745
VARS	-6.93822	-8.05306
EEF1G	-6.13795	-7.31046
KMT2A	-2.61213	-3.9066
RPS5	3.553587	2.46505
RPL5	2.673188	1.646299
RPS3	2.638967	1.546385
FARSB	2.461828	1.551497
RPS2	2.443886	1.320149
FHL3	2.268656	1.342084
RPL4	2.265216	1.287739
PRDX6	2.165308	1.202484
TNPO1	2.253471	1.108984
RPL8	2.09498	1.025901
NOP58	1.98363	1.119742
ACAT1	2.053364	0.983462
RPL7A	2.019287	1.010565
LLPH	1.087212	1.885158
HNRNPUL2-BSCL2;	2.002699	0.874478
RPL35A	1.911611	0.915504
RPS14	1.932471	0.86676
RPL14	1.908939	0.868244
RPS3A	1.944617	0.82938
CPSF1	1.763163	0.926144
PGAM5	1.798381	0.888874
NEFM	1.789243	0.881793
RPS8	1.825246	0.843491
RPL28	1.84022	0.770248
RPL21	1.84937	0.735727
ENO1	1.785864	0.790423
RPS13	1.805436	0.7643
SAP18	1.742427	0.815406
RPS4X	1.809334	0.728728

	Fold change (Log2)	
Gene name	Bait normalised	MLR normalised
RPL13A	1.805868	0.713027
RPS27	1.751548	0.765991
KPNA2	1.709574	0.788982
RPS11	1.752172	0.73054
RPS9	1.784788	0.697645
HMGA1	1.792662	0.688741
EEF2	1.723167	0.703827
SRSF6	1.628464	0.767132
RPL30	1.185843	1.206601
SRP72	1.676206	0.704083
RPS7	1.717133	0.639744
DDOST	1.672959	0.613464
RSL1D1	1.635425	0.619999
RPL26	1.656099	0.535884
SSRP1	1.510289	0.658438
SLU7	1.528104	0.573113
PDCD6	-0.51105	-1.5839
KIF21A	1.59971	0.482717
STOML2	1.358155	0.708756
LBR	1.50039	0.554587
RANBP1	1.578624	0.463749
PAICS	1.372918	0.655804
RBM28	1.240622	0.785508
DDX3X; DDX3Y	1.524089	0.50026
RPS15A	1.45722	0.558429
GMPS	1.462789	0.539015
RPN1	1.519261	0.471981
EHD1	0.988205	0.98744
HSP90AA1	1.535131	0.437101
RPL36-AHNRNPH2;	1.475431	0.441056
RPL38	1.316425	0.592517
DDX50	1.407688	0.453551
AKAP17A	1.360616	0.484124
PNN	0.426506	1.363454
PPP2R2A; PPP2R2C	1.339535	0.445536
TCEB3	0.767465	0.952573
LGALS1	1.205743	0.47737
PYCRL	-0.77824	-0.69642
EIF2S1	0.744631	0.719907

Supplementary Figure S2 (a) Sequences of the two repair templates used to engineer the D252H mutant mouse. Sequences corresponding to exonic regions of genomic DNA are capitalised. Areas that correspond to the gRNA sequences are in light blue, with PAM sites in dark blue. The amino acid change used to encode the D252H mutation is in red. **(b)** Weights and **(c)** Neuroscores of mice taken from the two D252H lines referred to as D252H.15 and D252H.16, at P21. t-tests showed no significant difference between lines in either weight (males p=0.77 t(9)=0.3 females p= 0.54 t(9)=-0.6) or neuroscore (males p=0.1 t(8)=1.8 females p=0.47 t(8)=-0.7).

a

mutated D252H template

TAAGGAAGGAAATGCAAGCGGCGTGTCCCTGCTGGAAGCCCTGGACACAAT
CCTGCCCCCCACCCGCCCTACTGACAAGCCCCTTCGTCTGCCTCTGCAGCA
TGTGTACAAGATTGGCGgtgagtgagggttcagtgctggggctcactgcgg
caggcgcttgcctactctgctccaaaccctgactaggatatcaacaa

Wildtype D252H template

TAAGGAAGGAAATGCAAGCGGCGTGTCCCTGCTGGAAGCCCTGGACACAAT
CCTGCCCCCCACCCGCCCTACTGACAAGCCCCTTCGTCTGCCTCTGCAGGA
TGTGTACAAGATTGGAGgtgagtgagggttcagtgctggggctcactgcgg
caggcgcttgcctactctgctccaaaccctgactaggatatcaacaa

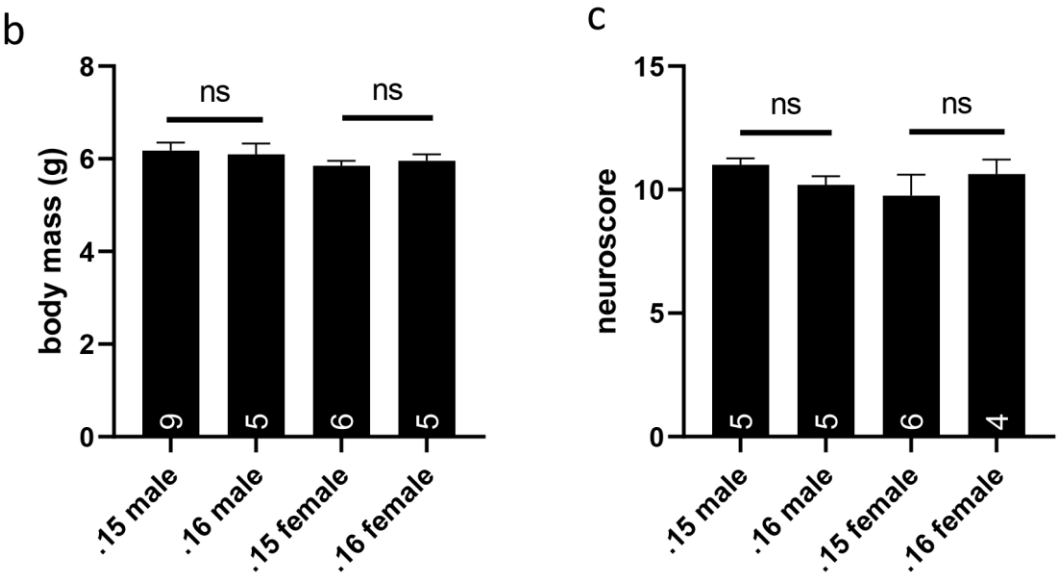

Supplementary Figure S3 Western blots of muscle lysates from wild type and D252H mutant mice and qPCR melt curves and standard curves. **(a)** muscle and **(b)** brain lysates showing eEF1A2 expression normalised to total protein levels. Each point on graph is data from a single mouse, over three technical replicates. eEF1A2 levels in male and female mice are not significantly different in either muscle **(a)** or brain **(b)** lysates (unpaired t-tests). **(c)** qPCR standard curves for eEF1A2 and reference genes GAPDH and Actin. Primer sets with R2>0.98 were considered acceptable for further

analysis.

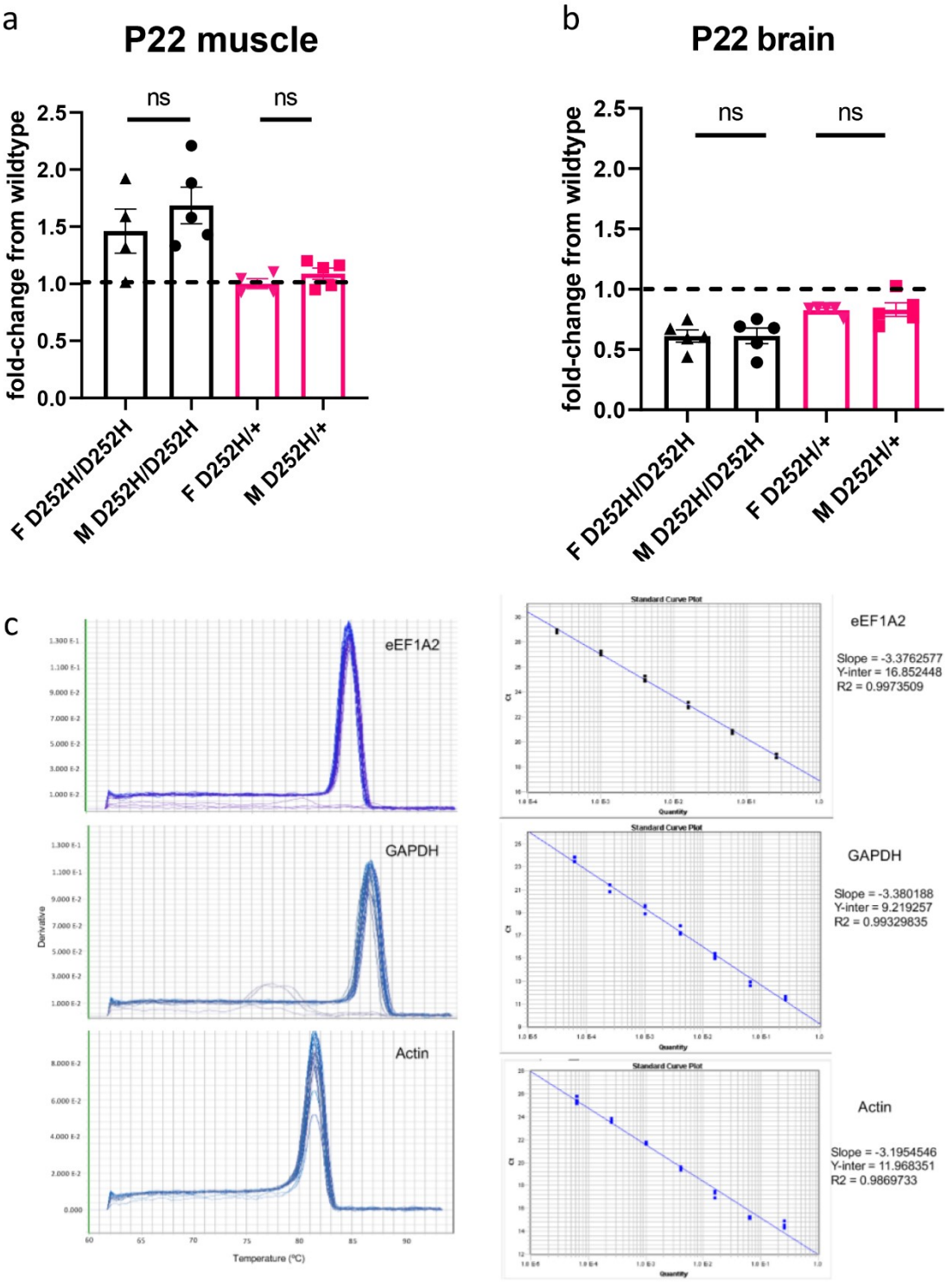
a
P22 muscle
ns
ns
fold-change from wildtype
2.5
2.0
1.5
1.0
0.5
0.0
F D252H/D252H
M D252H/D252H
F D252H/+
M D252H/+
b
P22 brain
ns
ns
fold-change from wildtype
2.5
2.0
1.5
1.0
0.5
0.0
F D252H/D252H
M D252H/D252H
F D252H/+
M D252H/+
c
eEF1A2
GAPDH
Actin
Derivative
Temperature (°C)
Standard Curve Plot
eEF1A2
Slope = -3.3762577
Y-inter = 16.852448
R2 = 0.9973509
Standard Curve Plot
GAPDH
Slope = -3.380188
Y-inter = 9.219257
R2 = 0.99329835
Standard Curve Plot
Actin
Slope = -3.1954546
Y-inter = 11.968351
R2 = 0.9869733

Supplementary Figure S4 Measurements of brain regions in D252H/+ mice. **(a)** example image of an H&E-stained brain section with hippocampus, dentate gyrus granule layer (DGgl) and the layers of the primary somatosensory area barrel field (SSp) annotated. At Bregma ± 0, the thickness of each cortical layer was measured in the primary motor area (MOp) and the primary somatosensory area barrel field (SSp). At Bregma -1.6 mm, the thickness of each cortical layer was measured in the primary somatosensory area barrel field (SSp), and the areas of the hippocampus and dentate gyrus granule layer (DGgl) were measured. Within each cortical area analysed, three separate measurements of each layer were taken per image and averaged. To control for tissue preparation artefacts, cortical layer thicknesses were then normalised to total cortical thickness, while hippocampus and DGgl areas were normalised to total hemisphere area. **(b)** male and **(c)** female MOp and SSp laminar compositions at three positions relative to Bregma. There is no significant difference in laminar composition between genotypes at any position (repeated measures one-way ANOVA). **(d)** Hippocampal area and **(e)** dentate gyrus granular layer (DGgl) area in male and female D252H/+ mice and wildtype littermates. There is no signficiant

difference between genotypes (repeated measures one-way ANOVA).

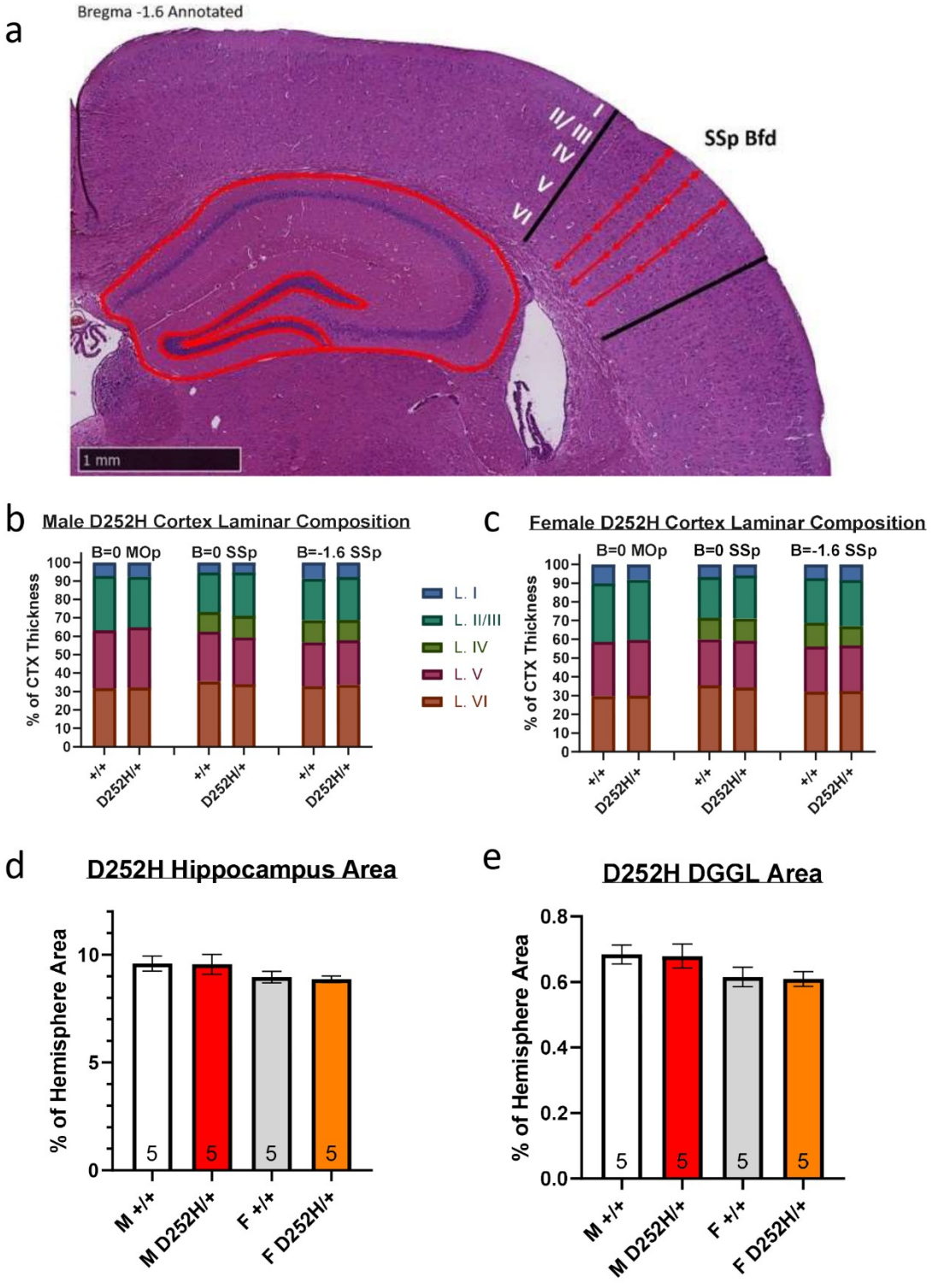

Supplementary Figure S5 Further behavioural tests on D252H/+ mice showed no significant differences from wild type littermates (a), (b) and **(c)** show results from the digging test in which mice were placed in a new cage containing 5cm bedding and observed for 3 minutes. **(d) (e)** show results from the nest building test in which mice were placed in a cage with a square of nestlet material and left overnight. The percentage of nestlet shredded (d) and the nest score (e) showed no significant difference between genotypes. **(f)** and **(g)** show further results from the open field test described in figure 5b. No significant difference is seen in the total distance travelled by each mouse (f) nor in the amount of time spent freezing (g). **(h)** Stranger mouse test stage 2. D252H/+ mice showed normal preference for social novelty as measure by time spent exploring a familiar mouse vs novel mouse.

(Two-way ANOVA showed significant effect of stimulus (novel vs familiar mouse) F(1,40)=33.66

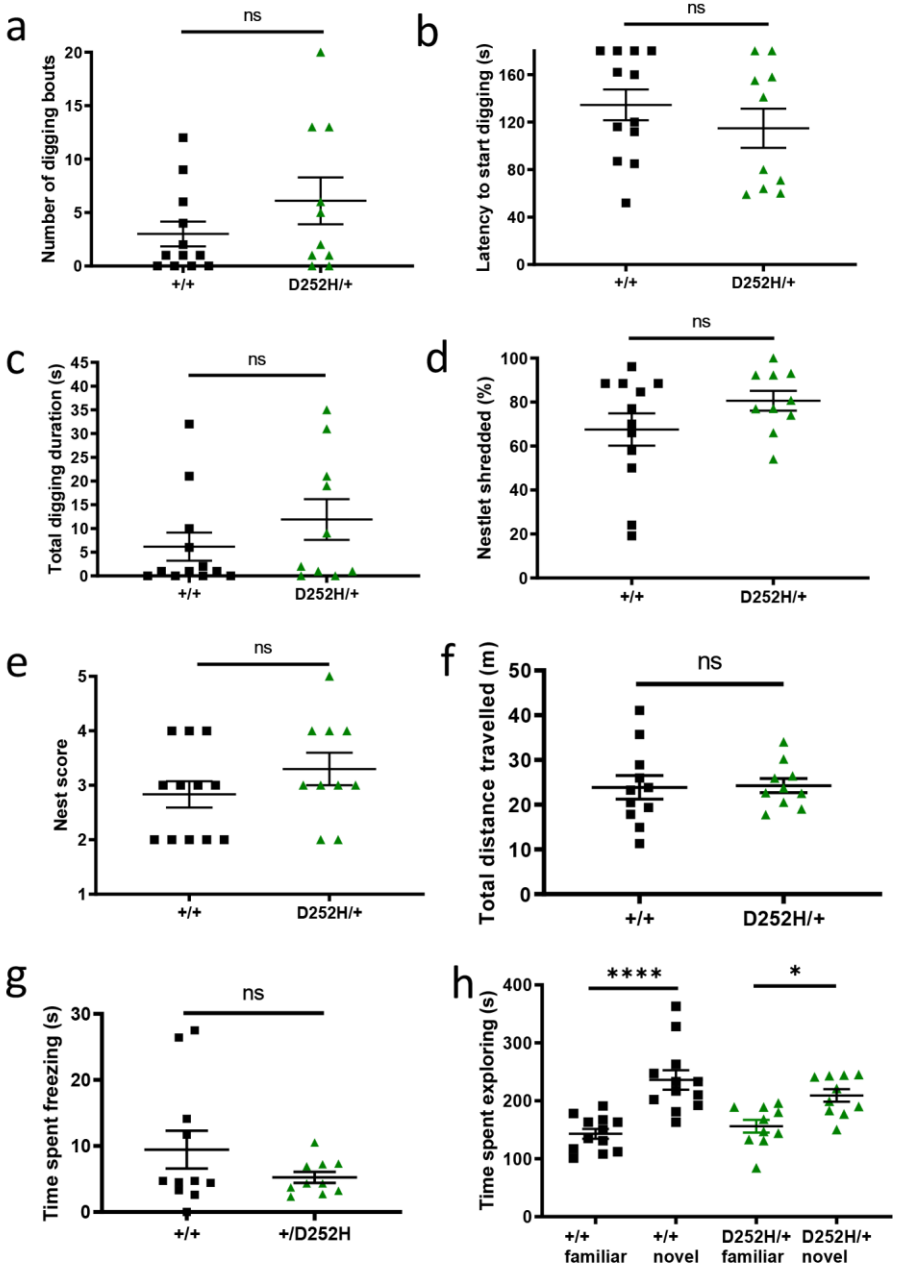

p,0.0001)

Supplementary Figure S6 Cervical and sacral spinal cord sections of P22 mice (a) stained against glial fibrillary acidic protein (GFAP) with strong staining indicated by arrows, **(b)** H&E-stained with vacuolated motor neurons indicated by arrows. White bar indicates 150um. Genotype of the mouse indicated in each image.

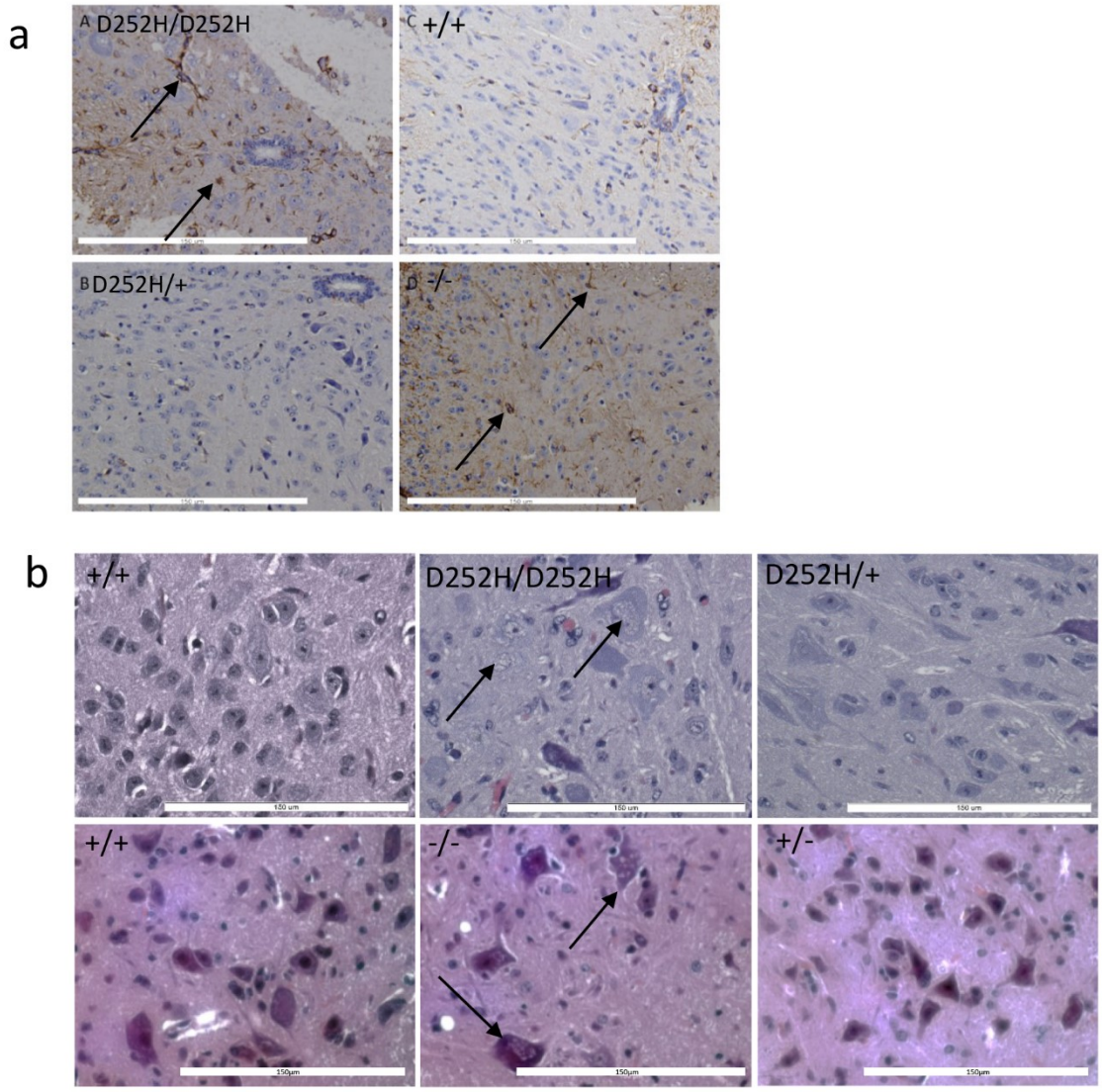

Supplementary Figure S7 *Eef1a2*$^{-/-}$ mouse sequence alignments and protein expression. **(a)** DNA alignment shows the 22bp deletion at the start of exon 3. The alignment of +/+ and -/- eEF1A2 protein sequences shows the premature stop codon introduced by the deletion, predicted to result in nonsense-mediated decay. **(b)** Western blot showing no expression of eEF1A2 in tissues taken from -/- mice using a primary antibody raised against amino acids 1-245 of eEF1A2. **(c)** a comparison of body weights of eEF1A2 null mouse lines between 14 and 25 days of age.

a

DNA alignment – region around deletion

```
eEF1A2+/+ ctacccttccagATGGGGAAGGGCTCTTTTAAATATGCCTGGGTGCTGGACAAGCTGAAG
eEF1A2-/- ctacccttccag----------ATGCCTGGGTGCTGGACAAGCTGAAG
```

Protein alignment – all coding exons

```
eEF1A2+/+ MGKEKTHINIVVIGHVDSGKSTTTGHLIYKCGGIDKRTIEKFEKEAAEMGKGSFKYAWVL
eEF1A2-/- MGKEKTHINIVVIGHVDSGKSTTTGHLIYKCGGIDKRTIEKFEKEAAEMPGCWTS*----

eEF1A2+/+ DKLKAERERGITIDISLWKFETTKYYITIIDAPGHRDFIKNMITGTSQADCAVLIVAAGV
eEF1A2-/- ------------------------------------------------------------

eEF1A2+/+ GEFEAGISKNGQTREHALLAYTLGVKQLIVGVNKMDSTEPAYSEKRYDEIVKEVSAYIKK
eEF1A2-/- ------------------------------------------------------------

eEF1A2+/+ IGYNPATVPFVPISGWHGDNMLEPSPNMPWFKGWKVERKEGNASGVSLLEALDTILPPTR
eEF1A2-/- ------------------------------------------------------------

eEF1A2+/+ PTDKPLRLPLQDVYKIGGIGTVPVGRVETGILRPGMVVTFAPVNITTEVKSVEMHHEALS
eEF1A2-/- ------------------------------------------------------------

eEF1A2+/+ EALPGDNVGFNVKNVSVKDIRRGNVCGDSKADPPQEAAQFTSQVIILNHPGQISAGYSPV
eEF1A2-/- ------------------------------------------------------------

eEF1A2+/+ IDCHTAHIACKFAELKEKIDRRSGKKLEDNPKSLKSGDAAIVEMVPGKPMCVESFSQYPP
eEF1A2-/- ------------------------------------------------------------

eEF1A2+/+ LX
eEF1A2-/- --
```

b

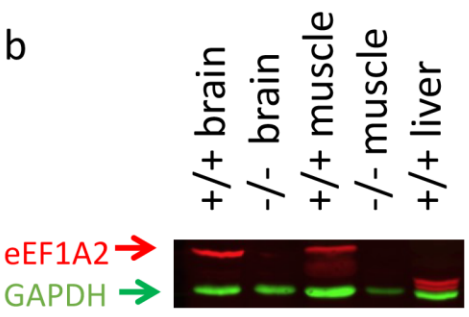

c

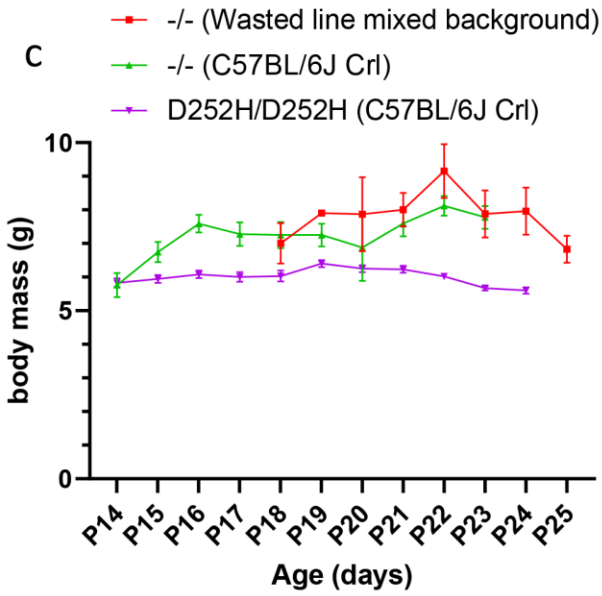

Supplementary Figure S8 Body mass and neuroscores of heterozygous null mice. (a) Male and **(b)** female body masses of heterozygous null (+/-) mice and wild type littermates between 3 and 22 days post birth. There is no significant difference between genotypes of either sex (repeated measures ANOVA). **(c)** male and **(d)** female neuroscores between 16 and 23 days post birth show no significant difference between +/- and wild type littermates (Repeated measures ANOVA). n=8-12 mice in each group.

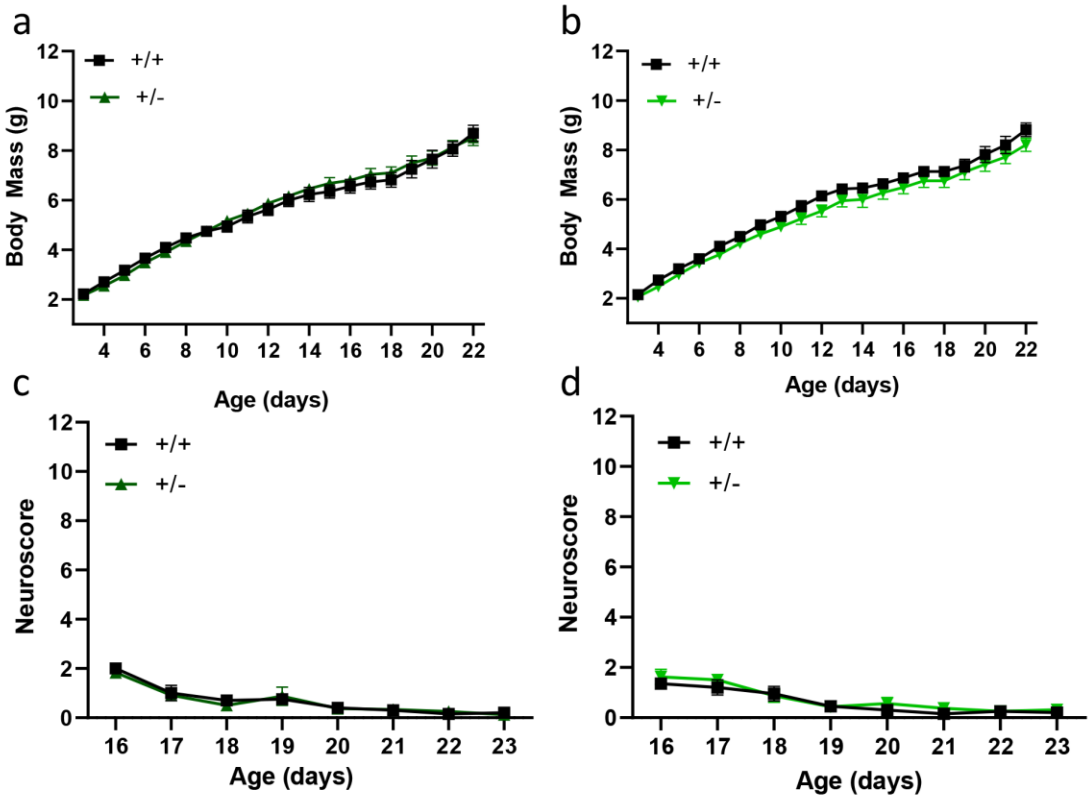

Abbreviations

DEE	developmental and epileptic encephalopathies
AEDs	anti-epileptic drugs
LFQ-MS	label-free quantification mass spectrometry
ssODN	single-stranded oligonucleotide
LFQ	label free quantification
MLR	most-likely ratio normalisation
qPCR	quantitative RT-PCR